JOURNAL OF GEOPHYSICAL RESEARCH, VOL. 97, NO. A7, PAGES 10,655–10,675, JULY 1, 1992

Kelvin-Helmholtz Instability at the Magnetospheric Boundary: Dependence on the Magnetosheath Sonic Mach Number

AKIRA MIURA

Department of Earth and Planetary Physics, University of Tokyo, Japan

It has recently been demonstrated, by means of a two-dimensional MHD simulation, that a finite thick velocity shear layer with super-Alfvénic velocity jump at the magnetospheric boundary is unstable to the Kelvin-Helmholtz (K-H) instability no matter how large the magnetosheath sonic Mach number (M_S); a result suggesting that the tail flank boundary of the magnetosphere is unstable to the K-H instability. In order to investigate this consequence further, the dependence of the development of the K-H instability on M_S is studied in detail. For all magnetosheath sonic Mach numbers a velocity boundary layer is formed by the instability inside of the magnetopause, and it becomes wider for a smaller magnetosheath sonic Mach number. A flow vortex is excited at the inner edge of the velocity boundary layer for all sonic Mach numbers, and the magnetopause boundary is more highly nonlinearly corrugated by the instability for a smaller sonic Mach number. The net energy and momentum flux densities into the magnetosphere are calculated just prior to the saturation stage; for $1.0 < M_S < 3.0$ the energy flux density into the magnetosphere is approximated by $0.054 M_S \rho_0 C_S^3/2 = 0.045 V_0 p_0$ (where ρ_0 is the unperturbed magnetosheath plasma density, p_0 is the unperturbed magnetosheath pressure, V_0 is the unperturbed magnetosheath flow velocity, and C_S is the magnetosheath sound speed), and the momentum flux density into the magnetosphere or the tangential (shearing) stress at the boundary is approximated by $0.083 p_0$. The anomalous viscosity by the instability decreases in the absolute magnitude with increasing M_S; this result suggests that the dayside (except the subsolar region) and the dawn-dusk magnetopauses, where the magnetosheath flow remains subsonic, are the most viscous parts of the boundary, although the tail flanks are also found to be viscous enough for the viscous interaction. The structure of the weak shock in the magnetosheath developed from the K-H instability and the asymptotic eigenmode structure of the instability are elucidated. The relevance of the simulation results to the viscous interaction and a ULF wave generation is finally discussed.

1. INTRODUCTION

It has long been suggested that the magnetospheric boundary between the solar wind and the stationary magnetospheric plasma is unstable to the Kelvin-Helmholtz (K-H) instability (*Dungey* [1955]; see also, *Chandrasekhar* [1961], *Gerwin* [1968], and *Southwood* [1979]), which is driven by the velocity shear at the boundary. *Boller and Stolov* [1970] were the first to suggest that the K-H instability at the magnetospheric boundary could possibly be a viscous interaction [*Axford and Hines*, 1961; *Heikkila*, 1990]. Since the nature of the viscous interaction by the K-H instability or the transport of momentum and energy by the instability is ultimately determined by its nonlinear process, the nonlinear treatment of the instability is essential in evaluating the nonlinear transport. It is only recently that the K-H instability at the magnetospheric boundary has been studied by nonlinear MHD simulations [*Miura*, 1982, 1984, 1987; *Wu*, 1986; *La Belle-Hamer et al.*, 1988; *Belmont and Chanteur*, 1989] and its importance in the viscous interaction has been quantitatively evaluated [*Miura*, 1984, 1987]. This instability has also been suggested as an important mechanism in exciting a ULF wave (Pc 5 (150–600 s) pulsation of a small azimuthal mode number ($m < 10$)) in the magnetosphere (e.g., *Atkinson and Watanabe* [1966]; see also recent reviews by *Southwood and Hughes* [1983] and *Allan and Poulter* [1984]).

Axford and Hines [1961] have suggested that a viscous interaction along the magnetospheric boundary can permit solar wind momentum to diffuse onto closed magnetospheric field lines. The resulting tailward convection flow would eventually be closed by an earthward return flow in the center of the tail, and a magnetospheric plasma convection (circulation) is formed inside the magnetosphere. The viscous contribution to the magnetospheric convection appears to be small in comparison with a reconnection-induced convection in the magnetosphere [*Reiff et al.*, 1981; *Wygant et al.*,1983; *Doyle and Burke*, 1983] (see also *Cowley* [1982]); nevertheless, the understanding of the nature of the viscous interaction at the magnetopause and the evaluation of its contribution to the magnetospheric convection are important for complete understanding of the solar wind–magnetosphere interaction. *Parker* [1958] suggested that the Fermi acceleration of ions at the disordered magnetopause gives rise to a not insignificant effective viscosity. *Axford* [1964] suggested the sound wave refraction mechanism at the magnetopause as a likely mechanism of the viscous interaction at the magnetopause. *Miura* [1982, 1984, 1987] has demonstrated that the K-H instability at the magnetospheric boundary is indeed an efficient viscous interaction at the boundary. The direct evidence of the viscous interaction seems to be the presence of the low-latitude boundary layer (LLBL) inside of the magnetopause, wherein the plasma is flowing tailward. Since a substantial portion of the LLBL is on the closed field lines [e.g., *Mitchell et al.*, 1987], the LLBL is connected to the ionosphere, and the flow energy in the LLBL is partly dissipated in the ionosphere as Joule heat [*Lemaire*, 1977; *Sonnerup*, 1980; *Nishida*, 1989]. Therefore, if there is no continuous replenishment of the antisunward flow momentum across the magnetopause, the antisunward flow in the LLBL should decay quickly with the distance

Paper number 92JA00791.
0148-0227/92/92JA-00791$05.00

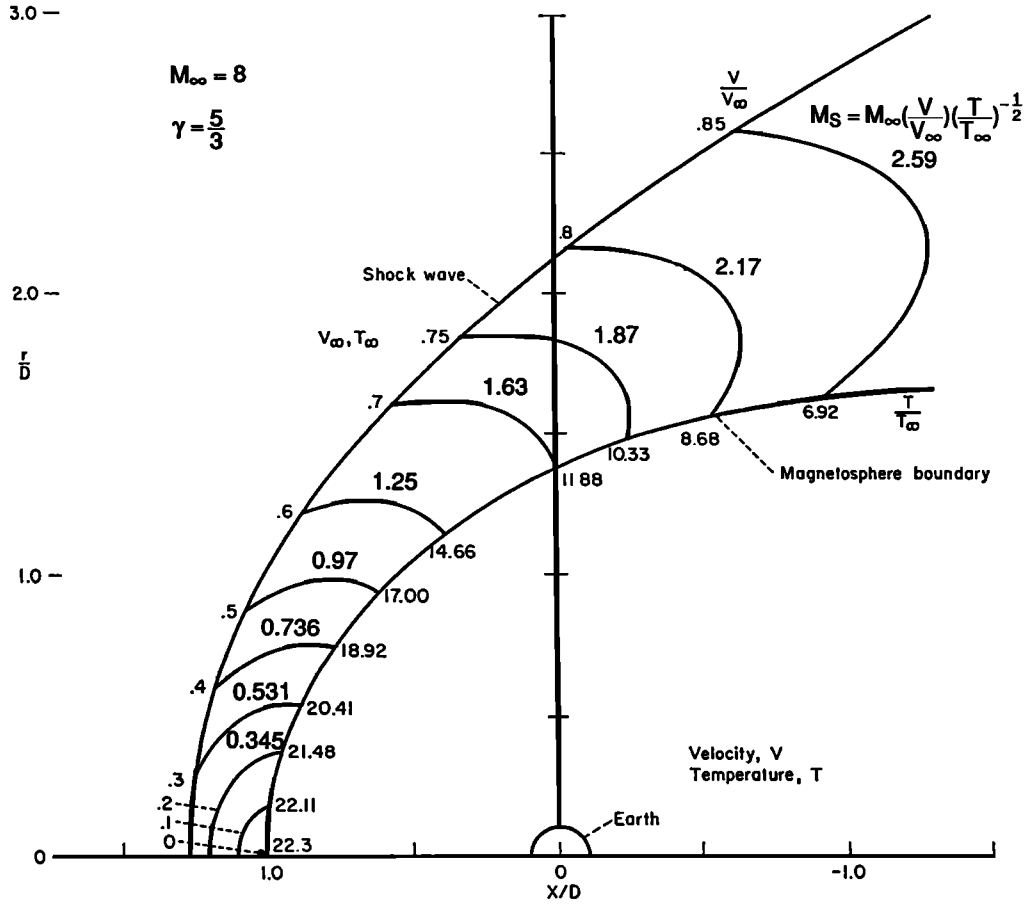

Fig. 1. Adapted from Figure 11 of *Spreiter et al.* [1966]. The local magnetosheath sonic Mach number M_S is added to their original figure.

along the magnetopause. Observations by *Hones et al.* [1972], however, show that a LLBL-like antisunward flow is present even within the tail flank boundaries, a fact suggesting that there is a continuous replenishment of the antisunward flow momentum across the tail flank boundary.

Quite a few investigations of the linear stability of the K-H instability in the compressible plasma (or fluid) were concerned with the hydrodynamic and MHD stability of the discontinuous vortex sheet (the velocity shear layer of zero thickness) [*Landau*, 1944; *Miles*, 1958; *Sen*, 1964; *Fejer*, 1964; *Talwar*, 1964; *Lerche*, 1966; *Southwood*, 1968; *Pu and Kivelson*, 1983*a*; *Prialnik et al.*, 1986]. According to most of these studies [*Landau*, 1944; *Miles*, 1958; *Sen*, 1964; *Fejer*, 1964; *Talwar*, 1964; *Pu and Kivelson*, 1983*a*; *Prialnik et al.*, 1986] there is an upper critical value of the Mach number above which two-dimensional waves propagating in the direction of the shear flow are stable; this suggests that a substantial portion of the tail flanks, where the magnetosheath flow is supersonic [*Spreiter et al.*, 1966] (i.e., the total velocity jump across the magnetospheric boundary minus the wave phase velocity is supersonic with respect to the sound velocity in the magnetosheath), must be stable to the K-H instability [e.g., *Sen*, 1965]. However, *Blumen et al.* [1975] and *Drazin and Davey* [1977] (see also *Lessen et al.* [1966]) have shown in the ordinary compressible fluid that for a smoothly varying velocity shear layer (the velocity shear layer of finite thickness) there is no such upper critical sonic Mach number and the smoothly varying velocity shear layer becomes unstable no matter how large the sonic Mach number.

By extending the previous simulation study of the subsonic K-H instability at the magnetospheric boundary [*Miura*, 1987] to an unexplored parameter regime, i.e., the tail flank boundary, where the magnetosheath flow is supersonic, it has recently been demonstrated [*Miura*, 1990; referred to hereinafter as M90] that the supersonic shear flow at the magnetospheric boundary with a smoothly varying velocity shear profile is unstable to the K-H instability no matter how large the magnetosheath sonic Mach number. This simulation result does suggest that the tail flank boundary is also unstable to the K-H instability. The purpose of the present study is to investigate this consequence further, in particular to investigate in detail the dependence of the K-H instability at the magnetospheric boundary on the magnetosheath sonic Mach number or the local time (because the sonic Mach number changes with the local time; see Figure 1) and to evaluate quantitatively the importance of the instability in the viscous interaction and in a ULF wave generation. An interesting consequence of the K-H instability for a high sonic Mach number shear flow, which we might well expect, is a shock formation [*Miura*, 1982, 1984; *Lele*, 1989; *Sandham and Reynolds*, 1990] (see also, *Norman et al.* [1982]); the present simulation also demonstrates where and how the shock evolves in the magnetosheath from the instability and the developed shock structure is elucidated in detail. The present study, along with the previous simulation

study [*Miura*, 1987], showing the dependence of the nonlinear evolution of the K-H instability, in particular the viscous transport, on the magnetosheath Alfvén Mach number, completes a two-dimensional MHD simulation study of the K-H instability at the magnetospheric boundary. The present study would also be helpful for understanding the stability and the consequences of the K-H instability in the solar wind [e.g., *Goldstein et al.*, 1990], at the Venus ionopause [e.g., *Wolff et al.*, 1980; *Thomas and Winske*, 1991], at the cometary ionopause [e.g., *Ershkovich and Mendis*, 1983], at the heliopause [e.g. *Fahr et al.*, 1986; *Baranov et al.*, 1991], and in the astrophysical applications such as the supersonic jets [e.g., *Norman et al.*, 1982; *Hardee*, 1983; *Norman and Hardee*, 1988] and the disk accretion [e.g., *Scharlemann*, 1978; *Ghosh and Lamb*, 1979; *Arons and Lea*, 1980; *Anzer and Börner*, 1980]. Although the work below is done for a special configuration of the terrestrial magnetospheric boundary, it does, however, have wider significance as a prototype of a number of similar problems in space physics and astrophysics.

Section 2 explains a flowing MHD equilibrium model of the low-latitude magnetospheric boundary, which had been used in previous studies [*Miura*, 1987, 1990]. Asymptotic eigenmode equations for the total pressure perturbation are derived in section 3. Simulation results are presented and discussed in section 4. Section 5 contains discussion of the implications of the simulation results in the solar wind–magnetosphere interaction and in a ULF wave generation. Section 6 gives a summary.

2. Model of Flowing Equilibrium

In the present simulation study a flowing MHD equilibrium model of the low-latitude magnetospheric boundary on the equatorial plane (see Figure 1 of M90) is used. Although the use of ideal MHD at the magnetopause is somewhat controversial by, for example, the finite ion Larmor radius effects, the anisotropic pressure effect [*Rajaram et al.*, 1991], and the invalidity of the frozen-in assumption [*Eastman*, 1979; *Lemaire and Roth*, 1991; *Fujimoto and Terasawa*, 1991*b*], a MHD approach is a necessary first step toward complete understanding of the K-H instability at the magnetopause. Since the driving mechanism of the K-H instability at the magnetospheric boundary is essentially hydrodynamic in nature (the electromagnetic force or the kinetic effect is not responsible for the instability), a MHD treatment of the K-H instability seems to be sufficient for clarifying the physics of its linear growth, the nonlinear saturation, and the momentum and energy transport by the instability. As far as these features are concerned, results of the hybrid simulations of the K-H instability by *Thomas and Winske* [1991] and *Fujimoto and Terasawa* [1991*a*] are similar to the results of the previous MHD simulations, although the plasma transport [*Thomas and Winske*, 1991] and the ion mixing [*Fujimoto and Terasawa*, 1991*a*] due to the nonideal MHD effects are new features demonstrated by those hybrid simulations. In MHD simulations of the K-H instability by *Tajima and Lebouef* [1980] and *Wang and Robertson* [1984] they assumed that the velocity shear layer has zero thickness. Such an initial value approach is known to be improperly posed [*Richtmyer and Morton*, 1967; *Nepveu*, 1980], and the linearly fastest growing mode is not accurately represented, although the nonlinear development of the unstable mode seems to be more or less correctly represented. Also *Lister et al.* [1988] emphasized the importance of preservation of the Galilean invariance during the simulation of the K-H instability.

In the present model of the finite thick magnetospheric boundary (Figure 1 of M90), both the flow velocity and the magnetic field are sheared across the magnetopause. For simplicity the thicknesses of the velocity shear layer and the magnetopause (magnetic shear layer) are assumed to be equal. The unperturbed flow velocity in the y direction and magnetic field are expressed as follows:

$$v_{0y}(x) = (V_0/2)[1 - \tanh(x/a)] \tag{1}$$

$$B_{0y}(x) = (B_0/2)[1 - \tanh(x/a)] \tag{2}$$

$$B_{0z}(x) = (B_0/2)[(1 + \beta_{sh})/(1 + \beta_{sp})]^{1/2}[1 + \tanh(x/a)] \tag{3}$$

where V_0 is the total jump of the flow velocity across the magnetospheric boundary and β_{sh} and β_{sp} are the plasma β ($\beta = 2\mu_0 p_0/B_0^2$) in the magnetosheath and in the magnetosphere, respectively. The plasma pressure is taken to satisfy the total pressure balance. The plasma temperature is assumed to be uniform across the boundary. The magnetospheric magnetic field is perpendicular to the magnetosheath flow, and the magnetosheath magnetic field is parallel to the magnetosheath flow. Notice that the nonuniform $v_{0y}(x)$ requires a nonuniform electric field component $E_{0x}(x)$, but this satisfies the equilibrium condition $\partial \mathbf{B}/\partial t = -\text{curl}\,\mathbf{E} = 0$. The magnetosheath flow is characterized by the Alfvén Mach number $M_A = V_0/V_A$, and the sound Mach number $M_S = V_0/C_S$, where V_A and C_S are the Alfvén speed and the sound speed in the magnetosheath, respectively. β_{sh} is given by $(6/5)(M_A/M_S)^2$ and β_{sp} is 0.2. In the present magnetosheath configuration, where the magnetic field is parallel to the flow, the sound Mach number is equal to the fast Mach number for $\beta_{sh} > 1$, because the fast mode speed parallel to the magnetic field is equal to the sound speed for $\beta_{sh} > 1$. The unperturbed plasma pressure in the magnetosheath p_{sh} and that in the magnetosphere p_{sp} are related to each other by $p_{sp}/p_{sh} = \rho_{sp}/\rho_{sh} = (1 + \beta_{sh}^{-1})/(1 + \beta_{sp}^{-1})$, where ρ_{sp} and ρ_{sh} are unperturbed plasma densities in the magnetosphere and in the magnetosheath, respectively. A periodic boundary condition is imposed at $y = 0$ and $y = L_y$. In the x direction we have placed boundaries at $x = \pm 10a$. The boundary condition in the x direction is such that there is no mass flow ($v_x = 0$) across the boundaries at $x = \pm 10a$. It then follows from ideal MHD equations that B_x and derivatives with respect to x of the remaining quantities (ρ, v_y, v_z, B_y, B_z, p) must vanish at the boundaries ($x = \pm 10a$), where ρ, $\mathbf{v}$, $\mathbf{B}$, and p are the plasma mass density, bulk velocity of the plasma, magnetic field, and plasma pressure, respectively. The two-step Lax-Wendroff method [*Richtmyer and Morton*, 1967] with an artificial viscosity term [*Lapidus*, 1967] is used to solve MHD equations. Time is normalized by $2a/V_0$.

3. Asymptotic Eigenmode Equation

For the finite thick velocity shear layer shown in Figure 1 of M90, the growth rate of the K-H instability is peaked at a wavelength comparable to 2π multiplied by the thickness of

the velocity shear layer [*Ong and Roderick*, 1972; *Walker*, 1981; *Miura and Pritchett*, 1982; *Mishin and Morozov*, 1983]. For a realistic set of $2a$ (thickness of the velocity shear layer) and V_0 at the magnetopause the fastest growing mode has a wave period of Pc 4 to Pc 5 range (45–600 s). This is the basis for considering the possibility of the K-H instability for the finite thick velocity shear layer as an excitation mechanism of the Pc 5 toroidal mode resonance in the magnetosphere.

In considering the K-H instability at the magnetopause, it should be noted that the magnetosheath flow changes from subsonic in the dayside to supersonic at the flank [*Spreiter et al.*, 1966] (*Parker* [1958] also pointed out this fact); this can be seen in Figure 1, which shows the local sonic Mach number M_S in the magnetosheath for different local time (Figure 1 was adapted from Figure 11 of *Spreiter et al.* [1966]). It is well known that the discontinuous vortex sheet (velocity shear layer of zero thickness) becomes unstable to the K-H instability only when V_0 lies between two critical velocities. The lower critical velocity for the two-dimensional wave propagating in the direction of the shear flow is determined by the Alfvén speed defined by using the magnetic field component parallel to the flow. Therefore, the total velocity jump must be super Alfvénic with respect to the magnetic field component parallel to the flow. The upper critical velocity for the two-dimensional wave propagating in the direction of the shear flow is of the order of the sound speed [*Landau*, 1944] for the hydrodynamic case and the fast magnetosonic speed for the MHD case [e.g., *Sen*, 1964]. Whereas for the finite thick velocity shear layer, there is no such upper critical velocity and the shear layer becomes unstable no matter how large the sonic Mach number [*Blumen et al.*, 1975; *Drazin and Davey*, 1977]. In considering an unstable K-H wave at the magnetopause, which has a finite tailward phase velocity V_{ph}, an important Mach number, which characterizes the intrinsic compressibility of the flow, is the convective Mach number M_c [*Papamoshou and Roshko*, 1988], which is the Mach number in a frame of reference convecting with the phase velocity of the unstable K-H wave. This convective Mach number is also important for discussing the shock formation by the K-H instability, because its value in the upstream is equal to the shock Mach number (see section 4.3).

For the low latitude boundary model of Figure 1 of M90 the asymptotic form of the linear eigenmode equation for the total pressure perturbation δp^* at $x \ll -a$ in the magnetosheath becomes [*Miura and Pritchett*, 1982]

$$\frac{d^2\delta p^*}{dx^2} - \kappa_{sh}^2 \delta p^* = 0 \tag{4}$$

where

$$\kappa_{sh}^2 = k_y^2 - \frac{\Omega^2}{[1 - (k_y^2 V_{A_{sh}}^2/\Omega^2)]C_S^2 + V_{A_{sh}}^2}$$

$$= -\frac{(\Omega^2 - k_y^2 C_S^2)(\Omega^2 - k_y^2 V_{A_{sh}}^2)}{(\Omega^2 - k_y^2 V_{A_{sh}}^2)C_S^2 + \Omega^2 V_{A_{sh}}^2} \tag{5}$$

and

$$\Omega = \omega - k_y V_0 = \omega_r + i\gamma - k_y V_0 \tag{6}$$

k_y being the wavenumber in the y direction. For the medium wavelength mode satisfying $\omega_r = O(k_y V_0/2) \gg |\gamma|$, $|\Omega_r| = |\omega_r - k_y V_0| \gg |\gamma|$ is satisfied and therefore

$$\text{Re}\,(\kappa_{sh}^2) = -\frac{(\Omega_r^2 - k_y^2 C_S^2)(\Omega_r^2 - k_y^2 V_{A_{sh}}^2)}{(\Omega_r^2 - k_y^2 V_{A_{sh}}^2)C_S^2 + \Omega_r^2 V_{A_{sh}}^2} \tag{7}$$

$$\text{Im}\,(\kappa_{sh}^2) = -2\gamma\Omega_r \frac{\Omega_r^4 (C_S^2 + V_{A_{sh}}^2)}{\{(\Omega_r^2 - k_y^2 V_{A_{sh}}^2)C_S^2 + \Omega_r^2 V_{A_{sh}}^2\}^2} \tag{8}$$

where $V_{A_{sh}}$ is the Alfvén speed in the magnetosheath. Furthermore, if $\beta_{sh} \gg 1$, one obtains

$$\text{Re}\,(\kappa_{sh}^2) = k_y^2 (1 - M_{c_{sh}}^2) \tag{9}$$

where the magnetosheath convective Mach number $M_{c_{sh}}$ is defined by

$$M_{c_{sh}} = -\Omega_r/(k_y C_S) = (V_0 - \omega_r/k_y)/C_S \tag{10}$$

This convective Mach number characterizes the nature of the magnetosheath disturbance as subsonic or supersonic. If $\beta_{sh} \gg 1$ and $M_A \gg 1$, one also has

$$\text{Im}\,(\kappa_{sh}^2) = -2\frac{\gamma\Omega_r}{C_S^2} \tag{11}$$

Therefore, for $\beta_{sh} \gg 1$ and $M_A \gg 1$, one obtains

$$\kappa_{sh}^2 = k_y^2 (1 - M_{c_{sh}}^2) - 2i\frac{\gamma\Omega_r}{C_S^2} \tag{12}$$

Notice that this expression is also valid for an unmagnetized plasma.

From (4) and (12) it is obvious that $M_{c_{sh}} > 1$ gives an oscillatory mode at $x \ll -a$ with a wavelength $\lambda_{x_{sh}}$ in the x direction given by

$$\lambda_{x_{sh}} = \frac{\lambda}{(M_{c_{sh}}^2 - 1)^{1/2}} = \lambda \tan\theta_{sh} \tag{13}$$

where θ_{sh} is the magnetosheath Mach angle defined by

$$\sin\theta_{sh} = 1/M_{c_{sh}} \tag{14}$$

and λ is the wavelength in the y direction parallel to the unperturbed flow. Equation (13) will be checked by using the simulation results for supersonic shear flows in section 4.1.

The eigenmode equation at $x \gg a$ in the magnetosphere becomes [*Miura and Pritchett*, 1982]

$$\frac{d^2\delta p^*}{dx^2} - \kappa_{sp}^2 \delta p^* = 0 \tag{15}$$

where

$$\kappa_{sp}^2 = k_y^2\left(1 - \frac{\omega^2}{k_y^2 C_F^2}\right) \tag{16}$$

and C_F is the fast magnetosonic speed in the magnetosphere defined by $C_F = (C_S^2 + V_{A_{sp}}^2)^{1/2}$, $V_{A_{sp}}$ being the Alfvén velocity in the magnetosphere. For the medium wavelength mode satisfying $\omega_r \gg |\gamma|$ one obtains

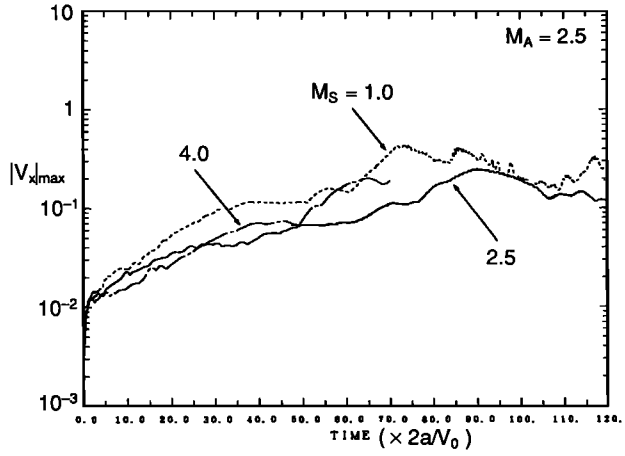

Fig. 2. Temporal evolution of the peak of $|v_x|$ normalized by V_0 for three different sonic Mach numbers M_S and a fixed Alfvén Mach number ($M_A = 2.5$).

$$\kappa_{sp}^2 = k_y^2(1 - M_{c_{sp}}^2) - 2i\frac{\gamma\omega_r}{C_F^2} \tag{17}$$

where the magnetospheric convective Mach number $M_{c_{sp}}$ is defined by

$$M_{c_{sp}} = \omega_r/(k_y C_F) \tag{18}$$

This convective Mach number characterizes the nature of the magnetospheric disturbance as subfast or superfast. If we express the e-folding distance of δp^* in the magnetosphere by $l_{x_{sp}}$, this is expressed by

$$l_{x_{sp}} = \frac{\lambda}{2\pi(1 - M_{c_{sp}}^2)^{1/2}} \tag{19}$$

Therefore, in the incompressible limit ($C_F \to \infty$ and $M_{c_{sp}} \to 0$) the evanescent eigenmode has an e-folding distance k_y^{-1} in the magnetosphere. Equation (19) will be checked by using the simulation results in section 4.1.

4. Simulation Results

4.1. *Growth of Perturbations for Supersonic Shear Flows*

A MHD simulation is initiated by adding a small seed of unstable perturbation to the flowing equilibrium described by equations (1)–(3). The small seed of unstable perturbation is so chosen that it has a peak velocity $|v_x|$ equal to $0.005V_0$ and a wavelength equal to L_y. For all simulation runs performed in the present study, the same wavenumber k_y of the unstable K-H mode, which satisfies $2k_y a = 0.8$, is used. This wavenumber is nearly equal to the wavenumber of the fastest growing (dominant) unstable mode. Using this k_y, the periodicity length L_y is expressed by $L_y = 2\pi/k_y = 15.7a$.

Figure 2 shows temporal evolutions of the peak of the x component of the flow velocity $|v_x|$ normalized by V_0 for three different magnetosheath sonic Mach numbers M_S = 1.0, 2.5, and 4.0 and for $M_A = 2.5$. β_{sh} in the magnetosheath are 7.5, 1.2, and 0.47, respectively, and ρ_{sp}/ρ_{sh} are 0.19, 0.31, and 0.52, respectively. The same temporal evolutions for eight different magnetosheath sonic Mach numbers M_S (0.5 ~ 5.0) and for $M_A = 10$ are shown in Figure 2 of M90. In that case, β_{sh} in the magnetosheath changes from 480 to 4.8 for M_S = 0.5 ~ 5.0 and ρ_{sh}/ρ_{sh} changes from 0.17 to 0.20. Figure 2 shows that for each sonic Mach number from 1.0 to ~4.0 the peak of the velocity perturbation $|v_x|$ normalized by V_0 grows linearly in the early phase and tends to saturate in a later period. The simulation for each sonic Mach number is terminated in the early phase of the nonlinear saturation for two reasons. One reason is that if the nonlinear development for the later phase is followed, numerical artifacts appear and the ideal MHD development of the K-H instability is affected by this numerical effect. A second reason is that in a real situation a nonlinear coalescence of the vortices, which is not allowed in the present simulation, arises after the saturation of the fastest growing mode. Hence further nonlinear development of the fastest growing mode after its nonlinear saturation does not seem to be realized in a real situation. Such a coalescence of vortices and resulting "inverse cascade" is demonstrated in a two-dimensional MHD simulation by *Belmont and Chanteur* [1989], which used a system size much longer than the wavelength of the fastest growing mode. The nonlinear coalescence of vortices excited by the K-H instability is also demonstrated by a two-dimensional hydrodynamic simulation of *Lele* [1989], a two-dimensional MHD particle simulation of *Tajima et al.* [1991], and two-dimensional electrostatic particle simulations of *Pritchett and Coroniti* [1984] and *Cai* [1991].

In the present case, shown in Figure 2, the magnetosheath magnetic field parallel to the magnetosheath flow is stronger than the case shown in Figure 2 of M90, and the unstable mode is more stabilized by the stronger tension force of the magnetic field lines. Therefore, for each sonic Mach number the amplitude of $|v_x|$ grows more slowly than the cases shown in Figure 2 of M90 for $M_A = 10$.

From the above observations it is evident that for fixed magnetosheath Alfvén Mach numbers M_A (=2.5 and 10.0), which are large enough so that the magnetic field is too weak to suppress the K-H instability, the model magnetospheric boundary shown in Figure 1 of M90 is unstable to the K-H instability no matter how large the magnetosheath sonic Mach number M_S. This result appears to be contradictory to the stability criterion for the discontinuous vortex sheet [*Landau*, 1944; *Miles*, 1958; *Sen*, 1964; *Fejer*, 1964; *Talwar*, 1964; *Pu and Kivelson*, 1983*a*; *Prialnik et al.*, 1986], which predicts that in the compressible plasma (or fluid) there is an upper critical Mach number above which the vortex sheet is stable to the two-dimensional perturbation propagating in the direction of the shear flow. The above result, however, is consistent with the linear analyses of *Blumen et al.* [1975], *Drazin and Davey* [1977], and *Choudhury and Lovelace* [1984] (see also *Lessen et al.* [1966]) showing that the smoothly varying shear layer is unstable for each value of the sonic Mach number. According to *Papamoshou and Roshko* [1988] this striking distinction between the stability of a vortex sheet and the stability of a finite thick velocity shear layer is quite elementary. Figure 3 is a diagram based on Figure 18 of *Papamoshou and Roshko* [1988], where distributions of the flow velocity (solid line) and the speed of the sound wave (dotted line) are drawn in stationary (or magnetospheric inertial) (left) and convective (right) frames of reference. *Papamoshou and Roshko*'s [1988] explanation is as follows: Perhaps the most elementary feature that distinguishes a supersonic flow from a subsonic one is that in

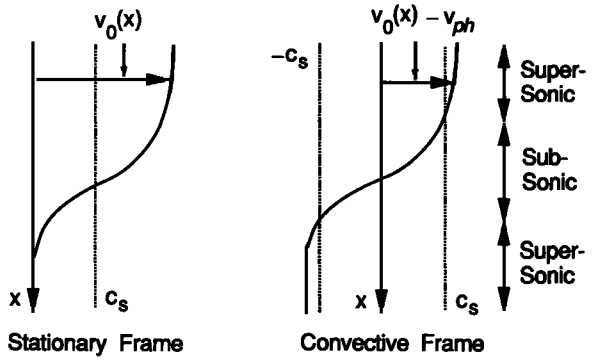

Fig. 3. A diagram based on Figure 18 of *Papamoshou and Roshko* [1988], where distributions of the flow velocity (solid line) and the sound velocity (dotted line) are drawn in stationary (magnetospheric inertial; left) and convective (with the phase velocity of the wave; right) frames of reference.

the supersonic case a disturbance does not propagate upstream and remains confined within a Mach cone, while in the subsonic case a disturbance is felt throughout the flow field. Given the limited region of influence of a supersonic disturbance, we might expect that a supersonic shear layer is more stable than a subsonic one. For supersonic shear flow with a finite thick shear layer as shown in Figure 3, however, there is a portion of the flow near the center of the shear layer where the local velocity, relative to the wave phase velocity, is subsonic. It is evident that the extent of this subsonic sublayer will decrease with increasing Mach number but will never vanish; this fact that in the compressible finite thickness shear layer there is always an imbedded subsonic region, thus a region potentially dominated by subsonic-type instabilities, is significant and is responsible for the fact that the shear layer of finite thickness remains unstable no matter how large the sonic Mach number.

The linear growth rates obtained from the slopes of the linear growth curves for $M_S = 0.5 \sim 2.5$ and $M_A = 10$ (Figure 2 of M90) are plotted in Figure 4 as a function of the sonic Mach number M_S. The linear growth rate is normalized by $V_0/2a$. It is obvious that the normalized linear growth rate decreases with increasing sonic Mach number for $0.5 < M_S < 2.5$ owing to the increase of the compressibility. This is consistent with the linear analysis of *Miura and Pritchett* [1982] and simulation results of *Lele* [1989] and *Sandham and Reynolds* [1990]. For $M_S = 3.0 \sim 5.0$ and $M_A = 10$, however, the normalized linear growth rates calculated from the average slopes of the linear growth curves in Figure 2 of M90 are nearly equal. Notice that *Gropengiesser* [1970] found that the linear growth rate tends to be nearly constant at high sonic Mach numbers in his calculation of the spatial amplification rate of the K-H instability for a finite thick velocity shear layer.

Figure 5 shows profiles along x of the total pressure perturbation δp^*, which are normalized by the unperturbed plasma pressure in the magnetosheath and averaged in the y direction over one wavelength for four different sonic Mach numbers (M_S) at their linearly growing stages; here, the perturbation $\delta F(t)$ is defined by $\delta F(t) = F(t) - F(t = 0)$. For all cases, δp^* in the magnetosphere are monotonous as is required from (15) and (17) and Figure 3 of M90 showing $M_{c_{sp}} < 1.0$. For $M_S = 1.0$ and $M_{c_{sh}} < 1.0$ (see Figure 3 of M90). δp^* in the magnetosheath is monotonous as is expected from (4) and (12). Figure 3 of M90 shows that $M_{c_{sh}} > 1.0$ for $M_S = 2.5$. Therefore (4) and (12) predict that δp^* in the magnetosheath is oscillatory. However, in this case, $M_{c_{sh}}$ is very close to 1.0, and hence the wavelength $\lambda_{x_{sh}}$ in the x direction of the magnetosheath oscillation of δp^* predicted by (13) is very large and longer than the distance from $x = 0$ to the boundary ($x = -10a$) in the magnetosheath side. Therefore, owing to the existence of the numerical boundary at $x = -10a$ the oscillation of δp^* can not be realized in the magnetosheath. For $M_S = 4.0$ and 5.0, Figure 3 of M90 shows $M_{c_{sh}} = 2.2$ and 2.8, respectively, and therefore (13) predicts that $\lambda_{x_{sh}}$ in the magnetosheath are $8.0a$ and $5.97a$, respectively. Figures 5*b* and 5*d* show that δp^* is indeed oscillatory in the magnetosheath, although only one cylce of the oscillation is allowed in the magnetosheath owing to the presence of the numerical boundary and the wavelength in the x direction is about $6.0a$ for both Figures 5*b* and 5*d*. This result agrees well with the predicted values of $\lambda_{x_{sh}}$. For all cases the total pressure perturbation δp^* shown in Figure 5 becomes zero near the magnetopause. This means that the unstable wave near the magnetopause is a slow-mode type. For $M_S = 4.0$, Figure 3 of M90 gives $M_{c_{sp}} \approx 0.7$. Therefore $l_{x_{sp}}$ given by (19) is $3.5a$. This predicted e-folding distance is nearly equal to the magnetospheric e-folding distance of δp^* for Figure 5*b*.

4.2. *Dependence on the Magnetosheath Sonic Mach Number*

The consequences of the K-H instability depend on the magnetosheath sonic Mach number M_S. Figure 6*a* shows the flow velocity vectors and Figure 6*b* shows the magnetic field vectors at quasi-saturation stages of the K-H instability for three different values of M_S and for $M_A = 10$. As M_S increases, the stabilizing effect of the compressibility increases and the normalized growth rate of the instability decreases (see Figure 4). Figure 6*a*(top) shows that the

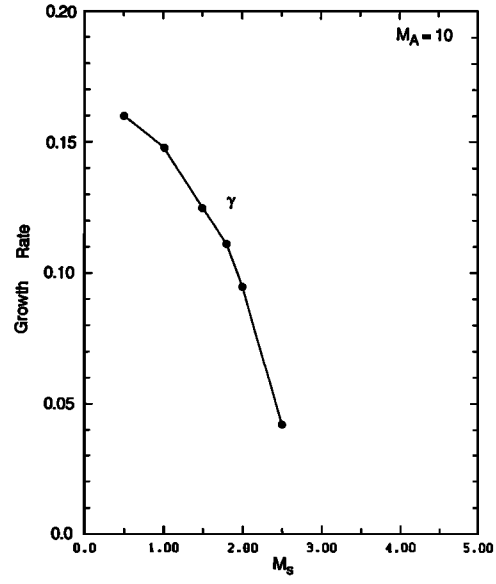

Fig. 4. Linear growth rates calculated from the slopes of the linear growth curves in Figure 2 of M90 as a function of the sonic Mach number M_S for $M_S = 0.5 \sim 2.5$ and $M_A = 10$. The growth rate is normalized by $V_0/2a$.

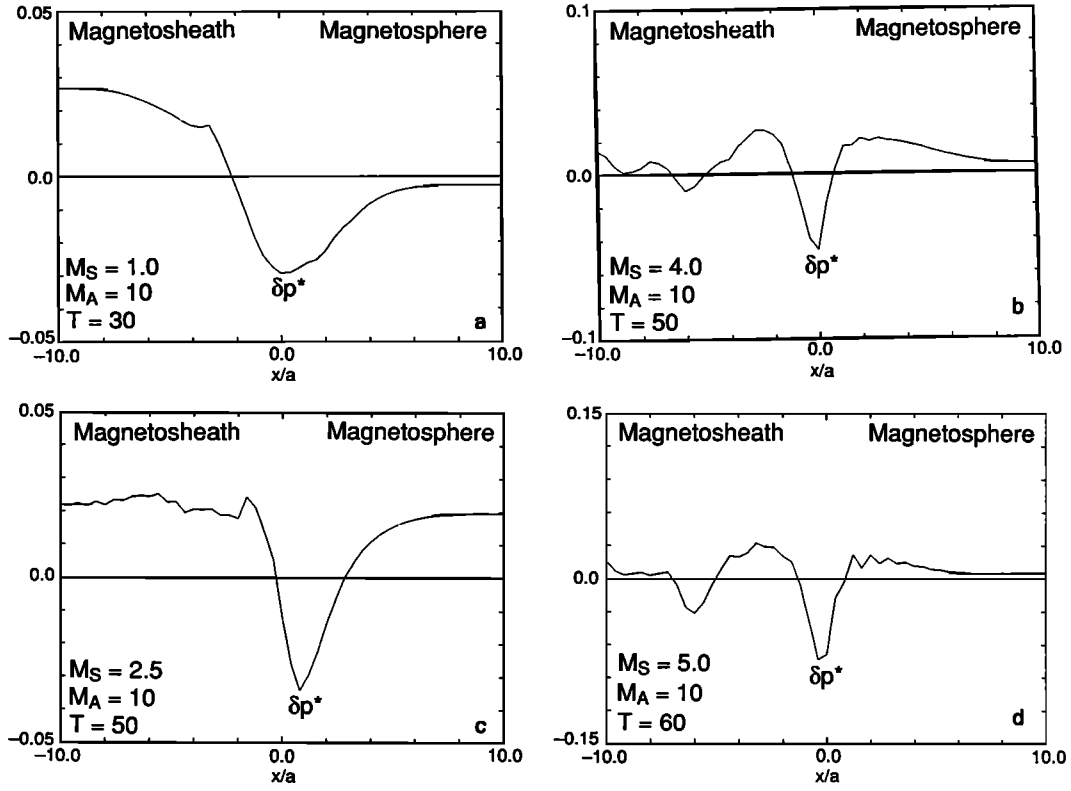

Fig. 5. Profiles along x of the total pressure perturbation δp^*, which are normalized by the unperturbed plasma pressure in the magnetosheath and averaged in the y direction over one wavelength for four different sonic Mach numbers M_S and for a fixed magnetosheath Alfvén Mach number $M_A = 10$ at their linearly growing stages.

initial flow velocity gradients are diffused quite markedly by the K-H instability at $T = 40$ for $M_S = 1$. However, for higher values of M_S, i.e., for $M_S = 2.5$ and 4.0, the flow velocity gradient is only slightly diffused (see Figure 6*a*, middle and bottom). Figure 6*b*(top) shows that for $M_S = 1.0$ the magnetopause boundary, characterized by a large gradient of the magnetic field strength, is corrugated highly nonlinearly. But this corrugation of the magnetopause boundary becomes less noticeable for higher values of M_S (see Figure 6*b*, middle and bottom). In Figure 6*b*(top and middle) the magnetic field just outside the magnetopause is intensified periodically by the flow pressing the magnetic flux and this process seems to be similar to the depletion process formulated by *Zwan and Wolf* [1976]. As will be shown later in Figure 8, such a periodic magnetic pressure increase seems to be associated with an antiphase plasma pressure change. Therefore this oscillation structure seems to be a slow mode type in nature. Although this structure seems to be related to the depletion process [*Zwan and Wolf*, 1976], the nature of this compressional oscillation is not clear at the present stage, and further study is necessary to clarify the origin of this oscillation.

Figure 7 shows streamlines for the same three cases as shown in Figure 6. The vortices are seen in all parts. For $M_S = 4.0$ (Figure 7*c*) the instability is weakest and the vortex is located at the inner edge of the velocity boundary layer, which is almost overlapped with the original magnetopause current layer near $x = 0$. However, as the sonic Mach number decreases, the instability becomes stronger, more plasma flow momentum in the magnetosheath is transported into the magnetosphere by the K-H instability, and a wider velocity boundary layer (VBL) is formed inside the magnetopause current layer (see Figure 7*a*). Therefore, as the sonic Mach number decreases, the vortex, which is located at the inner edge of the velocity boundary layer, tends to exist at the location of the larger positive x or at the location of the inner magnetosphere.

Figure 8 shows three-dimensional views of top surfaces of the plasma pressure distributions (Figure 8*a*) and magnetic pressure distributions (Figure 8*b*) at their quasi-saturation stages for three different values of M_S and $M_A = 10$. In this plot the height of the three-dimensional surface is proportional to the plasma or the magnetic pressure. As is required from the zeroth-order equilbrium the magnetic pressure is dominant in the magnetosphere, whereas in the magnetosheath the plasma pressure is dominant. For $M_S = 1$ the corrugation of the magnetopause boundary characterized by a large pressure gradient is quite distinct (see Figures 8*a* and 8*b*, top). For $M_S = 2.5$ and 4.0, however, the magnetopause boundaries are only slightly corrugated (see Figures 8*a* and 8*b*, middle and bottom). Instead, however, the magnetosheath plasma is more highly perturbed by compressional perturbations for higher values of the sonic Mach number M_S. As was seen in Figure 6, the magnetic pressure in the magnetosheath is oscillatory, particularly in Figure 8*b* (middle and bottom), and this oscillation seems to be associated with the corresponding antiphase oscillation of the plasma pressure shown in Figure 8*a*. Whether or not this oscillation in the magnetic pressure in the magnetosheath is a physical phenomenon is not certain, and further careful study seems

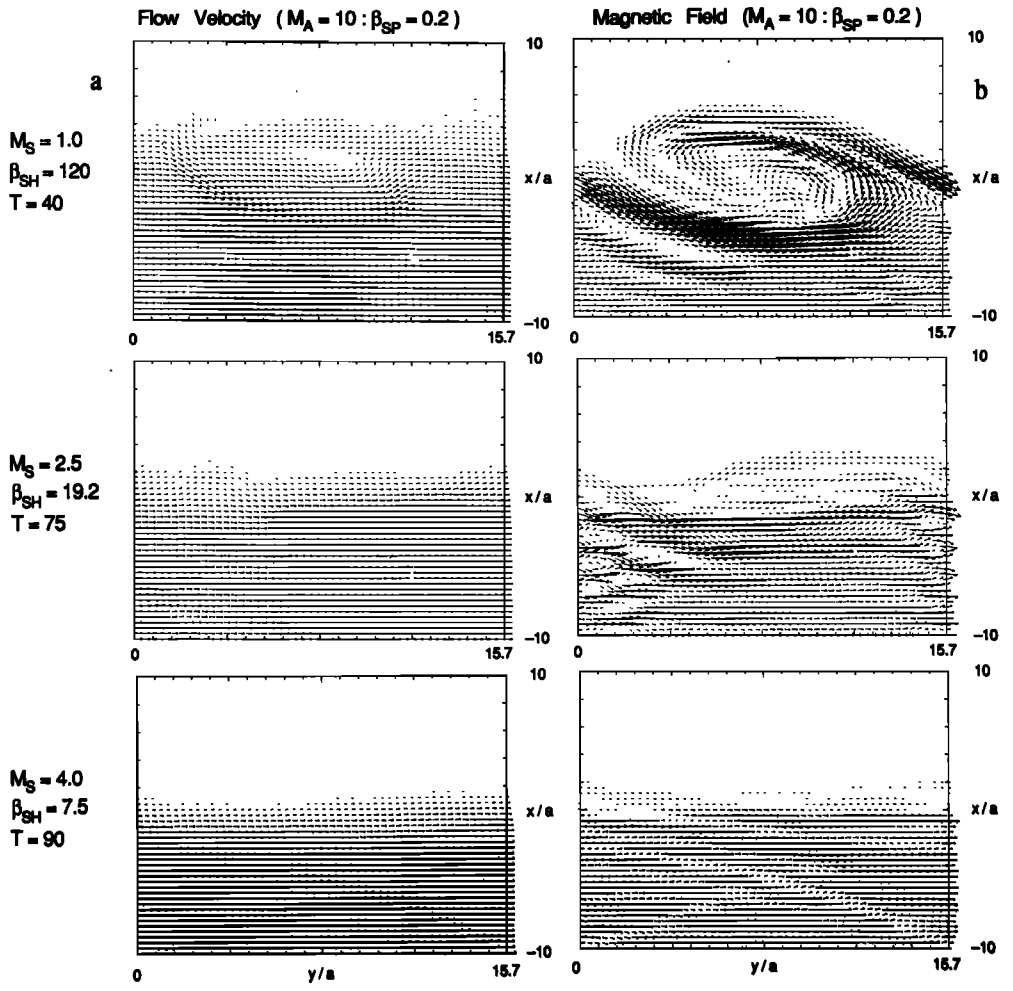

Fig. 6. (*a*) Flow velocity vectors and (*b*) magnetic field vectors at quasi-saturation stages of the K-H instability for three different values of M_S, i.e., M_S = 1.0, 2.5, and 4.0 from the top panels, and for M_A = 10.

to be necessary to identify the origin of this oscillation. Notice that this oscillation in the magnetosheath is different from the oscillation of δp^* in the magnetosheath shown in Figures 5*b* and 5*d*, which is predicted by (13) for the supersonic shear flow; Figure 5*b* gives $\lambda_{x,sh} \sim 6.0a$ for M_S = 4, but the wavelengths in the x direction of the oscillation shown in Figure 8*b*(middle and bottom) are much shorter than this.

Figure 9 shows three-dimensional views of top surfaces of the plasma pressure distributions (Figure 9*a*) and plasma density distributions (Figure 9*b*) at their quasi-stationary stages for three different values of M_S and M_A = 10. The corrugation of the magnetopause boundary characterized by a large density gradient near $x \sim 0$ is quite distinct for M_S = 1.0 (see Figures 9*a* and 9*b*, top); however, it is less clear for higher Mach number shear flows (see Figure 9*a* and 9*b*, middle and bottom). The compressional oscillations in the magnetosheath density distributions are seen for all cases. In Figure 9*b*(top) the amplitude of this oscillation is decreasing toward the numerical boundary at $x = -10a$, but in Figure 9*b*(middle) this oscillation seems to form a standing oscillation due to the existence of the wave reflected at the boundary ($x = -10a$). Therefore this oscillation appears to be a radiationlike structure radiated from the magnetopause, but again whether or not this oscillation in the density is a real physical phenomenon is not certain at the present stage. Further careful study is necessary to clarify the origin of this compressional oscillation in the magnetosheath, which was also seen in Figure 8. It should be pointed out here that such an oscillation in the magnetosheath was also found in Chantour's simulation of the K-H instability using a different numerical scheme [*Chanteur and Porteneuve*, 1989; G. Chanteur, private communication, 1991].

4.3. *Shock Formation*

Figure 10 shows three-dimensional views of top surfaces of the plasma pressures at four different times (T = 40, 50, 60, and 75) of the K-H instability for M_S = 2.5 and M_A = 10. Initially, the plasma pressure was uniform in the magnetosheath. At T = 40, however, the plasma pressure in the magnetosheath is undulated sinusoidally in the y direction. As time goes on, this pressure wave in the magnetosheath grows, and its leading edge becomes steeper and steeper (notice that in the frame of the magnetosheath flow the pressure perturbation is propagating in the negative y direction) because of the periodic deceleration and acceleration of the magnetosheath flow which cause the overtaking of the

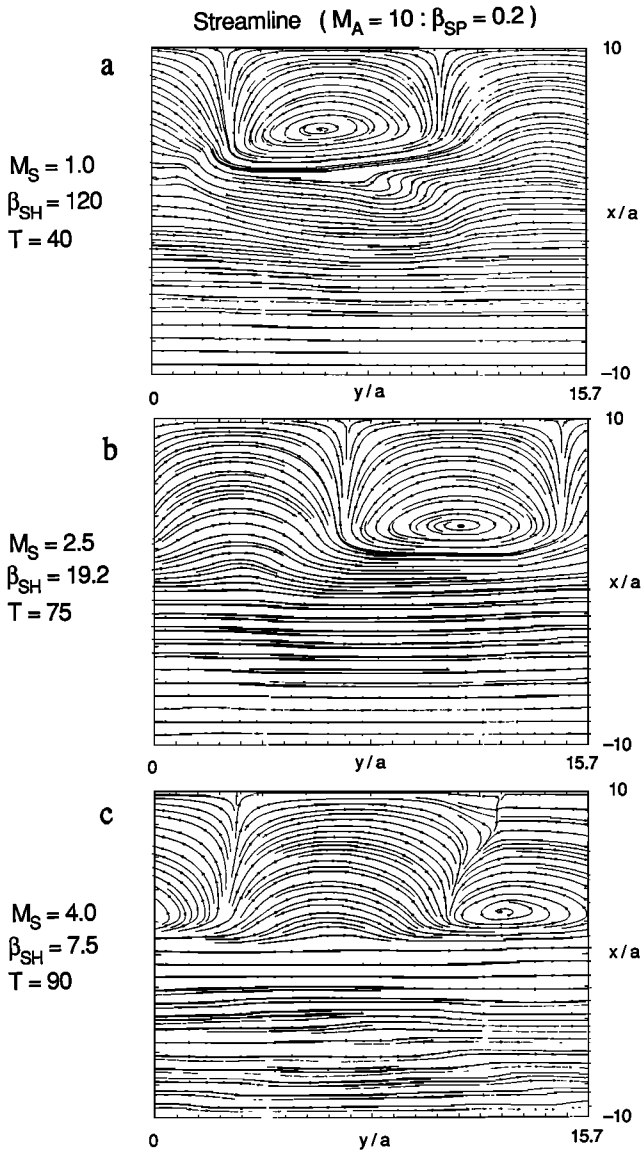

Fig. 7. Streamlines for the same three cases as shown in Figure 6.

decelerated flow by the accelerated flow. This nonlinear steepening of the leading edge continues until about $T = 60$, but after $T = 60$ this steepened structure seems to become steady. Since the plasma is compressed in the downstream, this steepened structure is shocklike in nature. In the present simulation a periodic boundary condition is used in the y direction. Therefore, in Figure 10 the upstream of the shocklike structure is connected to its downstream by the periodic boundary condition. In this sense the setting of the present simulation is not suitable for the study of shocks, because the upstream and the downstream of the shock must be completely separated by the entropy jump. However, the localized region near the shocklike structure in Figure 10 resembles a shock. Therefore, in the following, the Rankine-Hugoniot (R-H) relation is checked for the shocklike structure shown in Figure 10 in order to determine whether the shocklike structure is a real shock. Figure 10 shows that the normal to the shocklike structure is almost parallel to the y axis and is parallel to the flow direction. Since the magnetic field at the shocklike structure (see Figure 6*b*, middle) is parallel to the flow in the magnetosheath, the normal to the shocklike structure is parallel to the magnetic field. Therefore this shocklike structure resembles a parallel shock [*Hoffmann and Teller*, 1950]. Since $C_S > V_A$ is satisfied in the magnetosheath, for the present case, with $M_S = 2.5$ and $M_A = 10$, this parallel shocklike structure is gasdynamical in nature [*Bazer and Erickson*, 1959]. Therefore, in the following, the R-H relation of the gasdynamical shock is checked. In order to check the R-H relation the shock Mach number M_1 must be first calculated. In order to do this the speed of the wave frame (or the shock frame) in the y direction is calculated by plotting the position (trajectory) of the peak of the pressure perturbation at $x = -9.6a$ as a function of time in Figure 11 and by calculating the slope of the trajectory. Except in the initial phase ($0 < T < 20$), during which the initial unstable seed perturbation is adjusted to become an unstable eigenfunction of the K-H instability for the present parameter set, the pressure peak moves with almost constant speed, which is interpreted as the phase speed of the unstable perturbation. In Figure 10 a small undulation can be seen at $T = 50$ in the upstream of the shocklike structure and this undulation becomes much larger at $T = 60$ and 75. This undulation seems to be an unphysical numerical artifact, because the K-H instability is nondispersive. Consequently, the shock condition should be checked before this numerical artifact appears to become important. Therefore, in the following, the R-H relation is checked at $T = 50$, when the nonlinear steepening of the shocklike structure does not have a large unphysical oscillation in the upstream. From the slope of the y versus T curve in Figure 11 the phase speed $V_{ph} = 0.625V_0$ is obtained at $T = 50$.

Figure 12 shows the y component of the plasma flow velocity in the wave (shock) frame $u = v_y - V_{ph}$ and the sound speed $C_S = (\Gamma p/\rho)^{1/2}$ normalized by V_0, where Γ (=5/3) is the ratio of the specific heats, at $x = -9.6a$ and $T = 50$ as a function of y for $M_S = 2.5$ and $M_A = 10$ (notice that for $C_S > V_A$ the phase speed of the fast magnetosonic wave in the direction parallel to the magnetic field is C_S). From Figure 12 it is evident that the flow in the shock frame is supersonic in the upstream ($y < 5.2a$) and subsonic in the downstream ($y > 5.2a$) and is consistent with the presence of a gasdynamical shock. The minimum of sound speed occurs in the upstream at $y = 4.31a$. At this point the flow velocity is peaked and the Mach number (shock Mach number M_1) is 1.29. Figure 13 shows profiles as a function of y of the pressure p, the density ρ, the temperature T, the y component of the flow velocity v_y, and the y component of the magnetic field B_y at $x = -9.6a$ and $T = 50$. In the downstream of the shocklike structure, the pressure, the density, and the temperature are all increased, whereas the flow velocity is decreased; this is consistent with the presence of a gasdynamical shock. The magnetic field component B_y is almost constant across the shock layer as is required for the parallel shock. Although B_y is slightly undulated in the upstream region, this change of B_y is perhaps due to a mechanism, which is independent of the mechanism of the shock formation. Using the observed shock Mach number M_1, the ratios ρ_2/ρ_1, p_2/p_1, and u_2/u_1, where the subscripts 1 and 2 represent the upstream and the downstream, respectively, are calculated from the R-H relation:

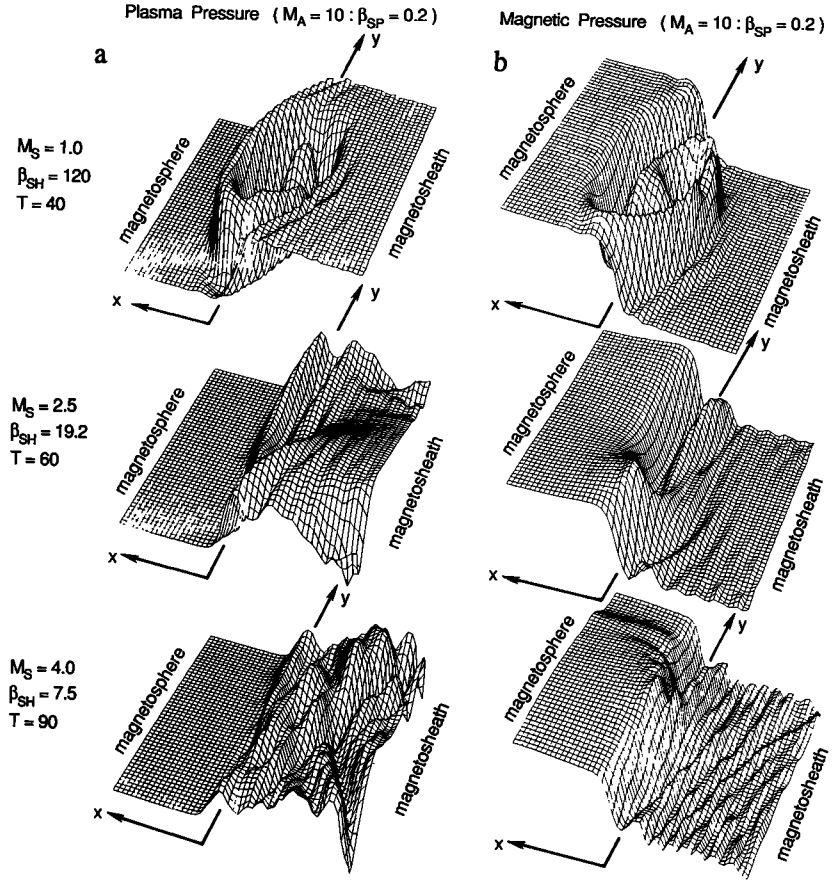

Fig. 8. Three-dimensional views of top surfaces of (*a*) the plasma pressure distributions and (*b*) magnetic pressure distributions at their quasi-saturation stages for three different values of M_S, i.e., M_S = 1.0, 2.5, and 4.0 from the top panels, and for M_A = 10.

$$\frac{\rho_2}{\rho_1} = \frac{(\Gamma + 1)M_1^2}{2 + (\Gamma - 1)M_1^2} \tag{20}$$

$$\frac{p_2}{p_1} = \frac{2\Gamma M_1^2 - (\Gamma - 1)}{\Gamma + 1} \tag{21}$$

$$\frac{u_2}{u_1} = \frac{2 + (\Gamma - 1)M_1^2}{(\Gamma + 1)M_1^2} \tag{22}$$

Table 1 summarizes those ratios obtained from the R-H relation using M_1. The observed values of ρ_2/ρ_1, p_2/p_1, u_2/u_1 calculated using the MHD quantities at $y = 4.31a$ (upstream) and $y = 7.85a$ (downstream), where ρ_2 and p_2 are peaked, in Figure 13 are also shown in Table 1. Table 1 shows that the R-H relationship is very well satisfied with errors of less than 5%. From this it is obvious that the localized shocklike structure shown in Figure 10 is a real shock discontinuity (weak shock). Notice that in the present ideal MHD scheme the dissipation mechanism necessary for the formation of the shock discontinuity is provided by the artificial viscosity introduced following *Lapidus* [1967].

4.4. *Energy and Momentum Transport by the Instability*

By taking a spatial average over one wavelength of the energy conservation equation [e.g., *Miura*, 1984]

$$\partial \varepsilon / \partial t = -\nabla \cdot \mathbf{Q} \tag{23}$$

where ε is the energy density defined by

$$\varepsilon = \tfrac{1}{2}\rho v^2 + \frac{1}{2\mu_0} B^2 + \frac{p}{\Gamma - 1} \tag{24}$$

and $\mathbf{Q}$ is the energy flux density defined by

$$\mathbf{Q} = \left(\tfrac{1}{2}\rho v^2 + \frac{\Gamma p}{\Gamma - 1}\right)\mathbf{v} + \frac{1}{\mu_0}\,\mathbf{E} \times \mathbf{B} \tag{25}$$

one obtains a spatially averaged energy conservation equation

$$\frac{\partial \langle \varepsilon \rangle}{\partial t} = -\frac{\partial \langle Q_x \rangle}{\partial x} \tag{26}$$

where $\langle Q_x \rangle$ is expressed by

$$\langle Q_x \rangle = \left\langle \left(\tfrac{1}{2}\rho v^2 + \frac{\Gamma p}{\Gamma - 1}\right) v_x + \frac{1}{\mu_0}\,(\mathbf{E} \times \mathbf{B})_x \right\rangle \tag{27}$$

Here the angle brackets represent the spatial average over one wavelength in the y direction. By taking a spatial average of the y component of the momentum conservation equation

$$\frac{\partial}{\partial t}\,\rho \mathbf{v} = -\nabla \cdot \left(\rho \mathbf{v}\mathbf{v} - \frac{1}{\mu_0}\,\mathbf{B}\mathbf{B}\right) - \nabla\left(p + \frac{1}{2\mu_0} B^2\right) \tag{28}$$

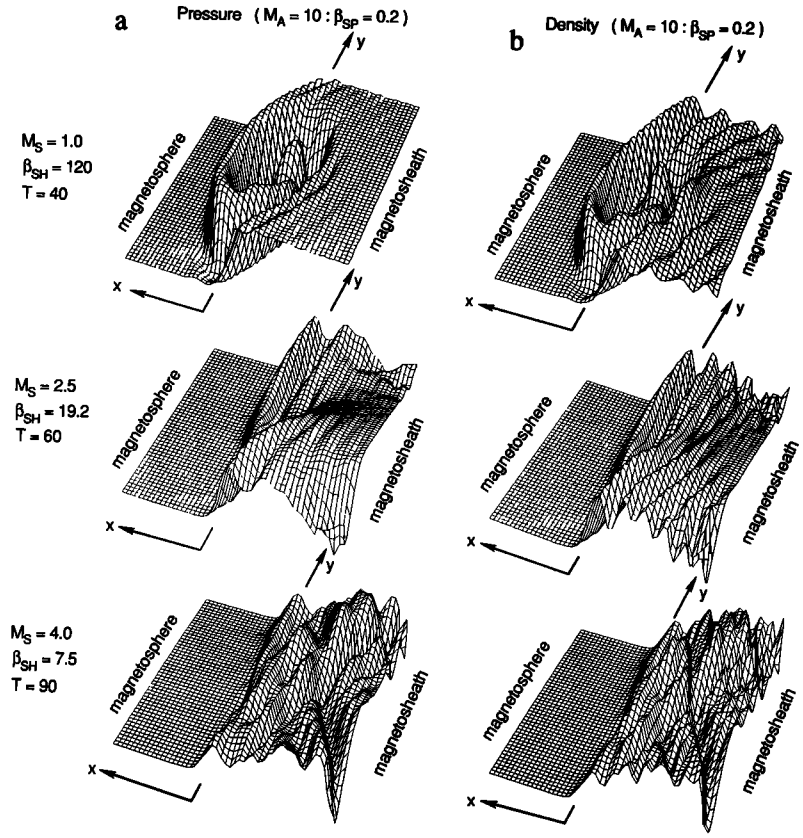

Fig. 9. Three-dimensional views of top surfaces of (*a*) the plasma pressure distributions and (*b*) the plasma density distributions at their quasi-stationary stages for three different values of M_S, i.e., $M_S = 1.0$, 2.5, and 4.0 from the top panels, and for $M_A = 10$.

one obtains, for the two-dimensional case ($\partial/\partial z = 0$) using the periodicity of perturbations in the y direction,

$$\frac{\partial}{\partial t}\langle \rho v_y \rangle = -\frac{\partial}{\partial x}\left\langle \rho v_x v_y - \frac{1}{\mu_0} B_x B_y \right\rangle \tag{29}$$

This means that the instability can exert a finite tangential stress $-\langle \rho v_x v_y - B_x B_y/\mu_0 \rangle$ on plasmas.

The energy flux density is calculated in the rest frame of the magnetosphere when the perturbation is still slightly growing just prior to the saturation and normalized by the

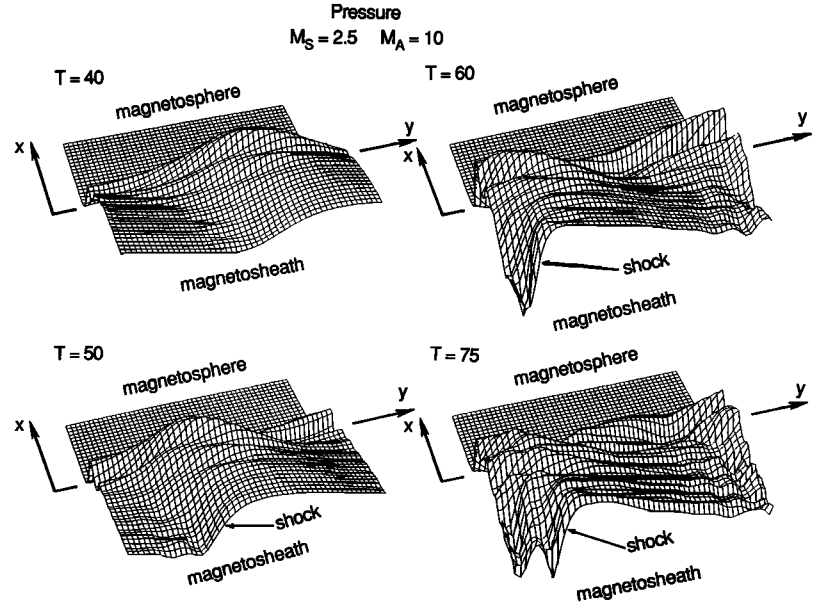

Fig. 10. Three-dimensional views of top surfaces of the plasma pressures at four different times of the K-H instability for $M_S = 2.5$ and $M_A = 10$.

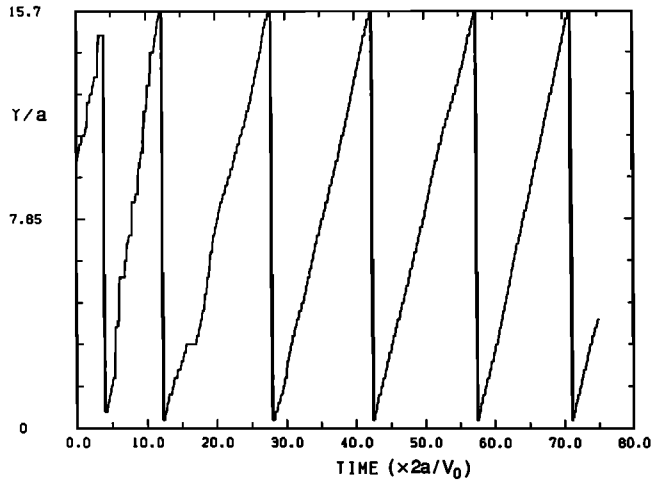

Fig. 11. Plot of the position of the peak of the pressure perturbation at $x = -9.6a$ as a function of time for $M_S = 2.5$ and $M_A = 10$.

magnetosheath kinetic energy flux density $\rho_0 V_0^3/2$, where ρ_0 is the unperturbed magnetosheath plasma density. Figure 6 of M90 shows profiles of each energy flux density (defined positive for the energy flux density into the magnetosphere) averaged over one wavelength for subsonic ($M_{c_{sh}} < 1$) and supersonic ($M_{c_{sh}} > 1$) shear flows. It was found that the peak of the total energy flux density, which is directed from the magnetosheath into the magnetosphere, occurs near $x = 0$, which is the initial boundary between the magnetosheath and the magnetosphere. Therefore the peak of the total energy flux density is a measure of the net energy transported from the magnetosheath into the magnetosphere by the K-H instability. Figure 14 shows the peak of the energy flux density into the magnetosphere normalized by the magnetosheath kinetic energy flux density $\rho_0 V_0^3/2$ as a function of M_S for $M_A = 10$. The normalized peak energy flux density decreases with increasing M_S and approaches a constant value, 0.4%, for higher M_S (>4), which occurs at the tail flank. For $1.0 < M_S < 3.0$ the normalized peak energy flux density is approximated by $0.054 M_S^{-2}$ (the dashed line in

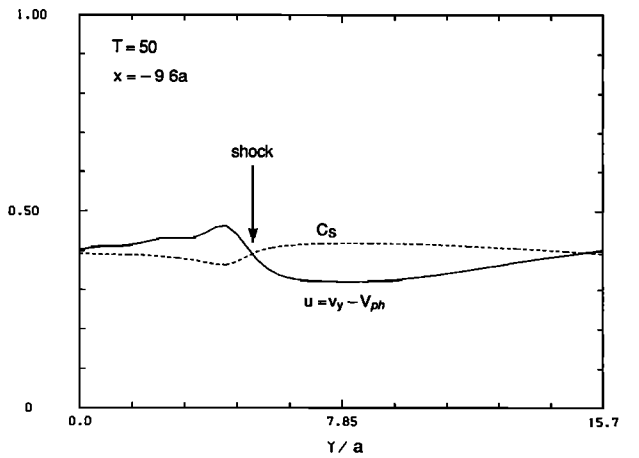

Fig. 12. The y component of the plasma flow velocity in the wave (shock) frame $u = v_y - V_{ph}$ and the sound speed $C_S = (\Gamma p/\rho)^{1/2}$ normalized by V_0, where Γ is the ratio of the specific heats, at $x = -9.6a$ and $T = 50$ as a function of y for $M_S = 2.5$ and $M_A = 10$.

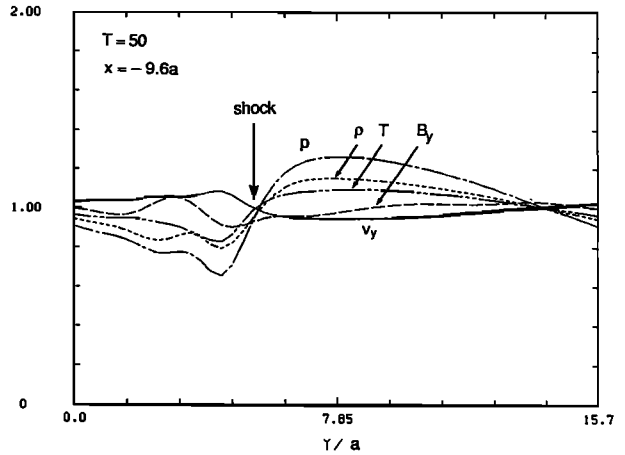

Fig. 13. Profiles as a function of y of the pressure p, the density ρ, the temperature T, the y component of the flow velocity v_y, and the y component of the magnetic field B_y at $x = -9.6a$ and $T = 50$ for $M_S = 2.5$ and $M_A = 10$. All quantities are normalized by their initial values.

Figure 14), and therefore the absolute peak energy flux density q is approximated by

$$q = 0.054 M_S^{-2} \rho_0 V_0^3/2 = 0.054 M_S \rho_0 C_S^3/2 = 0.045 V_0 p_0 \qquad (30)$$

where p_0 is the unperturbed magnetosheath pressure, for $1.0 < M_S < 3.0$. The fact that the normalized peak energy flux density tends to be constant for high M_S (>4) may be due to the fact that the saturation amplitudes of the instability are almost equal for high M_S (see Figure 2 of M90).

Figure 15 shows (from top) profiles in the x direction of spatial averages over one wavelength of the Reynolds stress $-\rho v_x v_y$ (solid line), the Maxwell stress $B_x B_y/\mu_0$ (dashed line), the x component of the electric field E_x (solid line), the plasma momentum in the y direction ρv_y (solid line), and the y component of the flow velocity v_y (solid line) at the quasi-saturation stage for $M_S = 2.5$ and $M_A = 10$. The stress (momentum flux density) is normalized by the magnetosheath flow momentum flux density $\rho_0 V_0^2$ and defined positive for the momentum flux density into the magnetosphere. Other quantities are so normalized that only relative scales are meaningful. The dashed lines in the profiles of E_x, ρv_y, and v_y show initial profiles of those quantities. The Reynolds stress reaches 0.8% of $\rho_0 V_0^2$ near the magnetopause, and the plasma momentum ρv_y in the magnetosheath is diffused from the magnetosheath into the magnetosphere (hatched region), where the large Reynolds stress is observed. Therefore the Reynolds stress is responsible for the momentum transport as (29) predicts. The Maxwell stress is much

TABLE 1. Observed Ratios of Densities, Pressures, and Velocities in the Shock Frame, The Ratios Calculated From the Rankine-Hugoniot Relation by Using the Shock Mach Number $M_1 = 1.29$, and the Relative Errors

	Observed	R-H Relation	Error, %
ρ_2/ρ_1	1.45	1.43	1.4
p_2/p_1	1.93	1.84	4.7
u_2/u_1	0.677	0.699	3.3

Subscripts 1 and 2 represent upstream and downstream, respectively.

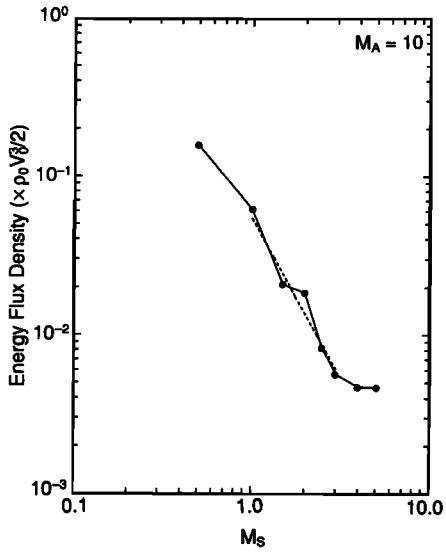

Fig. 14. Peak of the energy flux density into the magnetosphere normalized by the magnetosheath kinetic energy flux density $\rho_0 V_0^3/2$ as a function of M_S for $M_A = 10$. The dashed line is a power law fit $0.054\, M_S^{-2}$ for $1.0 < M_S < 3.0$.

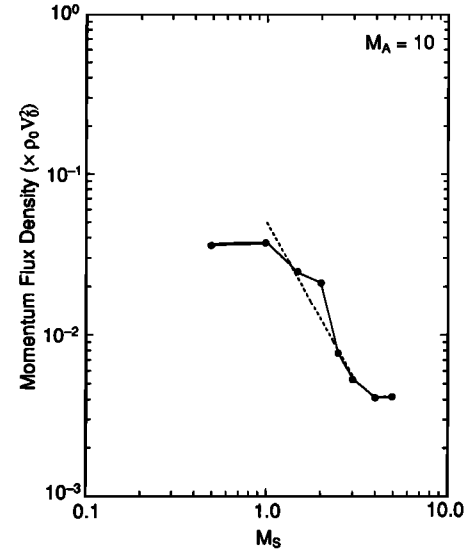

Fig. 16. Peak of the momentum flux density into the magnetosphere (tangential stress at the boundary) normalized by $\rho_0 V_0^2$ as a function of M_S for $M_A = 10$. The dashed line is a power law fit $0.05\, M_S^{-2}$ for $1.0 < M_S < 3.0$.

smaller than the Reynolds stress because $M_A \gg 1.0$ [*Miura*, 1987]. Also the magnitude of the electric field $|E_x|$ increases from the dashed line to the solid line where the large Reynolds stress is observed. Therefore the flow momentum flux in the y direction (antisunward direction) by $E_x \times B_z$ flow increases in the velocity boundary layer formed inside the magnetopause current layer. In order to evaluate the contribution of the K-H instability to the magnetospheric convection the spatial average over one wavelength of the convection potential difference (not necessarily electrostatic potential but just an integral of the electric field) across the boundary layer defined by $\int \langle E_x \rangle\, dx$ was calculated. The ratio of this integral of the electric field to its initial value was found to be 3.23; thus the antisunward convection voltage drop (strength) is amplified several times by the momentum transport associated with the K-H instability. Notice that for subsonic Mach numbers this ratio was found to be much larger [see *Miura*, 1987, Figure 9].

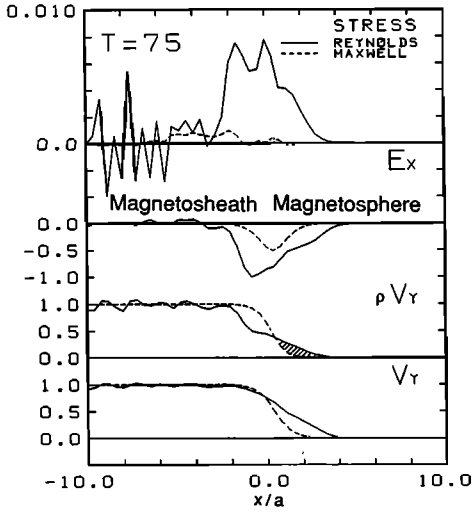

Fig. 15. Profiles in the x direction of spatial averages over one wavelength of the Reynolds stress $\rho v_x v_y$ (solid line), the Maxwell stress $B_x B_y/\mu_0$ (dashed line), the x component of the electric field E_x (solid line), the plasma momentum in the y direction ρv_y (solid line), and the y component of the flow velocity v_y (solid line) in the quasi-stationary stage for $M_S = 2.5$ and $M_A = 10$. The stress is normalized by the magnetosheath flow momentum flux $\rho_0 V_0^2$, and other quantities are so normalized that only relative scales are meaningful. The dashed lines in the profiles of E_x, ρv_y, and v_y show initial profiles of those quantities. The hatched region in the profile of ρv_y represents the net flow momentum transported from the magnetosheath into the magnetosphere by the K-H instability.

Figure 16 shows the peak momentum flux density (tangential stress) calculated in the rest frame of the magnetosphere where the perturbation is still slightly growing just prior to the saturation and normalized by $\rho_0 V_0^2$ as a function of M_S for $M_A = 10$. The normalized peak momentum flux density decreases with increasing M_S and approaches a constant value of 0.4% for higher M_S (>4), which occurs at the tail flank. For $1.0 < M_S < 3.0$ the normalized peak momentum flux density is approximated by $0.05 M_S^{-2}$ (the dashed line in Figure 16) and hence the absolute momentum flux density into the magnetosphere or the tangential (shearing) stress at the boundary τ is given by

$$\tau = 0.05 M_S^{-2} \rho_0 V_0^2 = 0.05 \rho_0 C_S^2 = 0.083 p_0 \qquad (31)$$

In order to see the dependence of the momentum transport on the magnetosheath sonic Mach number M_S more quantitatively the anomalous viscosity is defined according to the definition of the eddy viscosity in ordinary hydrodynamics [e.g., *Lamb*, 1945] as follows:

$$\nu_{ano} = -\frac{\langle \rho v_x v_y - \mu_0^{-1} B_x B_y \rangle}{d\langle \rho v_y \rangle / dx} \qquad (32)$$

The part of ν_{ano} by the Reynolds stress $-\rho v_x v_y$ is the eddy viscosity in ordinary hydrodynamics, and the part by the Maxwell (magnetic) stress $B_x B_y/\mu_0$ is the magnetic viscosity [e.g., *Eardley and Lightman*, 1975]. Figure 17 shows the dependence of the maximum anomalous viscosity at $x = 0$

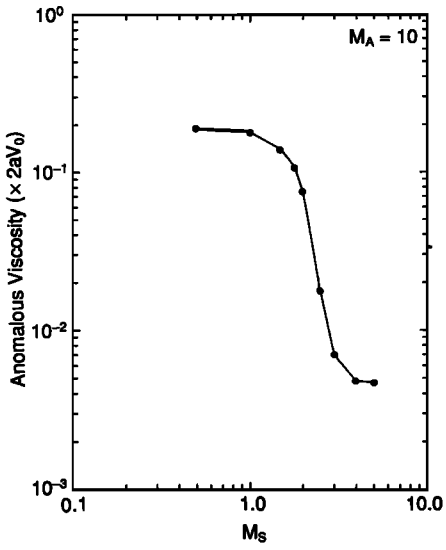

Fig. 17. Maximum normalized anomalous viscosity at $x = 0$ attained during the instability growth as a function of M_S for $M_A = 10$.

attained during the instability growth normalized by $2aV_0$ on the sonic Mach number M_S in the magnetosheath for $M_A = 10$. For $M_S \sim 1$, the anomalous viscosity takes a value of $\sim 0.2 \times 2aV_0$. However, as M_S increases the normalized anomalous viscosity decreases considerably and for $M_S > 3$ it approaches a constant value 0.005.

5. Discussion

In this section the simulation results in section 4 are discussed in the light of observational results in the solar wind–magnetosphere interaction and in a ULF wave generation.

5.1. *Growth of Perturbations for Supersonic Shear Flows*

Norman et al. [1982] have shown that the K-H instability occurs in their supersonic jet simulations. However, in their simulations the subsonic shear flow at the contact surface behind the bow shock seems to be responsible for the K-H instability. Therefore their simulations do not seem to have demonstrated that the supersonic shear flow is unstable to the K-H instability. Simulations of supersonic jets by *Norman and Hardee* [1988] have shown that the supersonic jet is unstable to the K-H instability. But according to linear analyses of the supersonic jet by *Gill* [1965] and *Hardee and Norman* [1988] the supersonic jet is unstable to the K-H instability even when the jet is separated from the surrounding medium by a vortex sheet owing to the fact that sound waves inside the jet are reflected back and forth. Therefore, as far as the linear stability is concerned, the stability of the supersonic jet does not seem to be relevant to the present simulation results showing that the finite thick velocity shear layer is unstable to the supersonic shear flow, although some of the nonlinear features of the supersonic jet simulation such as a shock formation are similar to the present simulation results.

The present study investigates further the results of M90 showing that the tail flank boundary of the magnetosphere, where the magnetosheath flow is supersonic, is unstable to the K-H instability. If we express the normalized growth rate by $\hat{\gamma}$, the actual growth rate γ is expressed in the denormalized form as $\gamma = \hat{\gamma}(M_S)V_0/2a = \hat{\gamma}(M_S)M_S C_S/2a$. If C_S and $2a$ are constant along the magnetopause from the dayside to the tail flank, the growth rate γ decreases in the absolute magnitude with increasing M_S for $M_S < 2.0$, because as shown in Figure 4, $\hat{\gamma}(M_S)$ decreases with increasing M_S much faster than M_S^{-1} for $M_S < 2.0$. Hence the growth rate of the instability at the tail flank becomes smaller than that in the dayside magnetopause owing to the compressibility. According to the present simulation results the dayside magnetopause boundary, where the convective sonic Mach number is less than 1.0, is highly nonlinearly corrugated by the K-H instability, whereas the magnetopause boundary at the tail flanks, where the convective sonic Mach number exceeds 1.0, is much less corrugated. Since $M_{c_{sh}} \sim 1.0$ occurs for $M_S = 2.5$ (see Figure 3 of M90), Figure 1 shows that this subsonic to supersonic transition of the K-H instability occurs at the magnetopauses of $\sim 30°$ behind the 0600–1800 LT meridian. Therefore, at the dayside and the dawn-dusk magnetopauses, a well-developed undulation and corrugation of the magnetopause boundary, as shown in the top panels of Figures 8 and 9, are expected to appear. This expectation is consistent with observations of *Lepping and Burlaga* [1979] (see also *Schardt et al.* [1984] for observation of the surface wave at Saturn's frontside magnetopause), although *Sckopke et al.* [1981] suggested that in their observation the magnetopause itself was stable to the K-H instability but the inner edge of the LLBL was unstable.

In the present simulation, only two-dimensional perturbations propagating in the direction of the shear flow have been considered. However, one should note that with three-dimensional disturbances, which propagate oblique to the shear flow, subsonic-type disturbances exist even at a very high Mach number [*Fejer and Miles*, 1963; *Lessen et al.*, 1965]. *Sandham and Reynolds* [1990] found in their three-dimensional linear analysis of the compressible mixing layer that oblique waves have a larger growth rate than the two-dimensional compressible mode above a convective Mach number of 0.6; namely, above a convective Mach number of 0.6, the mixing layer will have a strongly three-dimensional structure. In the case of the magnetopause, the magnetic field lines inside the magnetopause are tied to the conducting ionospheres. Owing to this coupling to the dissipative ionosphere the energy is not conserved during the growth of the K-H instability and the growth rate of the three-dimensional K-H instability is reduced. Therefore, whether the oblique three-dimensional mode has a larger growth rate than the two-dimensional compressible mode depends not only on the flow Mach number but also on the ionospheric Pedersen conductivity. Whether or not the three-dimensional development of the K-H instability at the magnetopause, including the line-tying effect of the ionosphere, is similar to the development of the three-dimensional mode in the fluid mixing layer [*Sandham and Reynolds*, 1991] is not certain at the present stage, and further study of the three-dimensional K-H instability, including the ionospheric line-tying effect, is necessary.

5.2. *Shock Formation*

An interesting and important finding of the present simulation of the supersonic shear flow is the spontaneous formation of shocks in the magnetosheath by the nonlinear

steepening of the leading edge of the unstable wave. Such a shock formation by the K-H instability may be relevant to the shock formation in the supersonic jet [*Norman et al.*, 1982]. For the present model configuration of the magnetospheric boundary (Figure 1 of M90), $C_S > V_A$ is satisfied in the magnetosheath, where the magnetic field is parallel to the magnetosheath flow. Therefore the present shock (Figures 10 and 13) formed in the magnetosheath by the K-H instability is a gasdynamical shock. If the magnetosheath magnetic field is perpendicular to the magnetosheath flow, then the K-H instability would lead to a formation of a fast perpendicular shock for a sufficiently high Mach number. Such a possibility has already been demonstrated in the case of uniform plasma for a subfast (more correctly, a subfast convective Mach number) shear flow [*Miura*, 1982, 1984]. In that case, a shock was formed from the subfast shear flow, because the flow was accelerated by the instability and the initial subfast shear flow became superfast in the development of the K-H instability. In an earlier brief discussion, *Miura* [1984] showed that the minimum subfast convective Mach number necessary for the appearance of the shock is about 0.65. It is interesting to note here that *Lele* [1989] and *Sandham and Reynolds* [1990] report in their simulations of the compressible K-H instability in the neutral fluid, that above $M_c = 0.7$ the flow develops shock waves (eddy "shocklets") embedded around the large-scale vortical structures. Therefore, for a high Mach number shear flow ($M_c > 0.7$) the formation of shocks seems to be an inevitable feature of the instability. These results of a shock formation by the K-H instability suggest that there are a series of "shocklets" formed in the magnetosheath adjacent to the magnetopause boundary at the tail flanks.

5.3. *Energy and Momentum Transport: A Viscous Interaction and Formation of a Velocity Boundary Layer*

The LLBL inside the magnetopause current layer is characterized by an antisunward flow on the closed field lines, the flow speed of which is smaller than the adjacent magnetosheath flow [*Eastman and Hones*, 1979]. Several mechanisms, which cause or require breaking down of the ideal MHD, have been proposed in order to explain the plasma penetration from the magnetosheath onto the closed field lines in the LLBL (e.g., impulsive penetration of the solar wind irregularities [*Lemaire*, 1977; *Heikkila*, 1982; *Lemaire and Roth*, 1991], anomalous particle diffusion by wave-particle interactions [*Eviatar and Wolf*, 1968; *Gary and Eastman*, 1979; *Tsurutani and Thorne*, 1982; *Gendrin*, 1983; *Berchem and Okuda*, 1990; *Treumann et al.*, 1991] and rereconnection of the open field lines with the closed field lines [*Nishida*, 1989], see also recent reviews by *Baumjohann and Paschmann* [1987], *Lundin* [1987] and *LaBelle and Treumann* [1988]). Whatever the mechanism of the plasma penetration is, a penetrated plasma with a tailward flow momentum is slowed down quickly with increasing distance along the magnetopause by the ionospheric Joule dissipation [*Lemaire*, 1977; *Sonnerup*, 1980; *Nishida*, 1989]. Observation by *Hones et al.* [1972], however, shows that a LLBL-like tailward flow is present even inside the tail flank boundaries, a fact suggesting that there must be a continuous replenishment of the tailward flow momentum across the tail flank boundary. The necessity of viscous stress imposed at the tail flank boundaries is also suggested by observation of the slowly tailward motion of the closed flux tubes in the distant geomagnetic tail [*Richardson et al.*, 1989]. *Owen and Slavin* [1991] have shown that the hypothetical viscous stress by the K-H instability at the deep tail boundary is 1 order of magnitude smaller than that required to explain the observed viscously driven plasma flows in the deep geomagnetic tail. This is a serious challenge to the K-H viscous interaction hypothesis. If we take into account the coalescence of the vortices which would cause much larger viscous stress by the instability, this problem may be resolved.

According to *Eastman* [1984] the kinetic energy flux associated with the tailward flow in the LLBL is about 70–400 GW, which is about 0.6–3.3% of Φ; here, Φ is the total kinetic energy flux of the solar wind flow incident on the magnetospheric cross section and is nearly equal to 1.2×10^4 GW. Although such an energy flux is small compared with a typical energy flux of ~800 GW required for substorm activities [*Baumjohann and Paschmann*, 1987], this energy flux is important for maintaining magnetospheric activities in the quiet condition. Figure 14 shows that the energy flux density by the K-H instability into the magnetosphere is ~15% of $\rho_0 V_0^3/2$ for $M_S = 0.5$ and 0.4% of it in the supersonic case. Although the normalized energy flux density into the magnetosphere by the K-H instability at the tail flank, where the flow is supersonic, appears to be smaller than that required for the viscous interaction, the normalized energy flux density at the dayside magnetosphere, where the flow is subsonic, is much larger than the required value. Therefore, on average, it seems that the normalized energy flux density into the magnetosphere by the K-H instability is large enough to replenish the plasma in the LLBL with the tailward flow kinetic energy of observed intensity.

Substitution of the Newtonian pressure formula given by $p_0 = p_{st} \cos^2 \psi$ [*Spreiter et al.*, 1966], where p_{st} is the unperturbed magnetosheath pressure at the subsolar point and ψ represents the angle between the directions of the free-stream velocity vector and the normal to the magnetosphere boundary, into (31) yields

$$\tau = 0.083 p_{st} \cos^2 \psi$$

for $1.0 < M_S < 3.0$. Therefore the tangential (shearing) stress by the K-H instability at the boundary, where $1.0 < M_S < 3.0$, is decreasing with the distance from the stagnation point along the magnetospheric boundary. It is interesting to notice that the linear relationship between the tangential (shearing) stress (τ) and the pressure (p_0) given by (31) is a standard assumption for the tangential (shearing) stress in the accretion disks ("α disks") [*Shakura and Sunyaev*, 1973], although the nature of the tangential stress or the viscosity is not well known. The present simulation result suggests that the shear (K-H) instability associated with the differential rotation in the accretion disks may give a required tangential stress, which is proportional to the pressure as shown by (31).

Figure 17 shows that the anomalous viscosity $\hat{\nu}_{ano}$ normalized by $2aV_0$ decreases with increasing M_S much faster than M_S^{-1}. Therefore ν_{ano} decreases with increasing M_S in the absolute magnitude. This result suggests that the K-H instability is more efficient as a viscous interaction at the dayside (except the subsolar region) and the dawn-dusk low-latitude boundary, where the convective sonic Mach number remains less than 1.0, than at the tail flank boundaries. If we

take $2a = 1000$ km and $V_0 = 500$ km/s as a typical parameter set at the tail flank, however, the anomalous viscosity ν_{ano} even at the tail flank becomes 2.5×10^9 m^2/s, which is comparable to that required for driving a magnteospheric convection in the magnetosphere [*Axford and Hines*, 1961]. The kinematic viscosity of the above order of magnitude is essential in the viscous LLBL-ionosphere coupling model of *Sonnerup* [1980], *Lotko et al.* [1987], and *Phan et al.* [1989], and in the high-latitude, low-latitude boundary layer model of the convective current system [*Siscoe et al.*, 1991].

Since the magnetic field component parallel to the flow is stabilizing the K-H instability by its tension force, the growth rate of the K-H instability at the magnetopause should depend on the dipole tilt angle χ, which is defined by the geomagnetic latitude of the subsolar point. With this notion, *Boller and Stolov* [1970] have suggested that the K-H instability is responsible for the observed semiannual variation of geomagnetic activity. *Maezawa and Murayama* [1986] have shown that the dependence of *AL* on the solar wind velocity V_{sw} varies with χ and its dependence is steeper when $|\chi|$ is small (see their Figure 9); the manner in which χ influences the effect of V_{sw} is consistent with the view that the K-H instability is responsible for the χ dependence of the geomagnetic activity, and hence the K-H instability at the magnetopause is a viscous interaction.

In the present model of the magnetospheric boundary the magnetic field component in the magnetosheath parallel to the magnetosheath flow gives a stabilizing contribution to the K-H instability. Therefore, when M_A, defined using the magnetic field component parallel to the magnetosheath flow, is less than ~2, the K-H instability is suppressed by the strong tension force of the magnetic field lines [*Miura and Pritchett*, 1982]. But if M_A exceeds ~2, the K-H instability occurs, the anomalous viscosity arises, and it tends to become a constant value for high M_A [*Miura*, 1987]. This suggests that there is a $|B_x|$ control of the K-H viscous interaction; namely, when the IMF $|B_x|$ is large, the K-H viscous interaction is suppressed, but for a small $|B_x|$ the K-H viscous interaction arises and the critical value of $|B_x|$, controlling the onset of the K-H viscous interaction, is determined approximately from $V_0/V_{A_{sh\|}} = V_0/|B_x|/(\rho_{sh}\mu_0)^{1/2} \sim 2.0$ (notice that in a uniform plasma the critical Alfvén Mach number defined by using the magnetic field component parallel to the flow is exactly equal to 2.0 [*Miura and Pritchett*, 1982], but in a nonuniform plasma the critical Mach number is ~2.0 [*Miura*, 1987]). For $n_{sh} \sim 10^7$ m^{-3} and $V_0 \sim 200$ km/s, $|B_x|_{cr}$ becomes ~15 nT. Using the results of extensive measurements of the viscous potential difference near local dusk [*Mozer*, 1984], *Reiff and Luhmann* [1986] calculated the average viscous potential difference as a function of the angle $\Theta_{sh} = \cos^{-1}(B_z/|B_{sh}|)$, where B_{sh} is the magnetic field component in the magnetosheath. They found a significant trend, from an average of 7.5 kV for angles less than 45°, to a nearly constant 1.5 kV for the other angles. This result, showing the $|B_x|$ control of the viscous interaction, is compatible with the K-H viscous interaction hypothesis, although the presence of the critical $|B_x|$ is not obvious in their analysis. The ground state of the magnetosphere under the IMF condition $B_y = B_z = 0$ and its dependence on B_x are currently investigated by *Nakagawa et al.* [1991].

5.4. *Penetration of the Poynting Flux Deep Into the Magnetosphere*

In both subsonic and supersonic cases the energy flux density, which penetrates deep into the magnetosphere, is dominated by the Poynting flux (see Figure 6 of M90). Therefore the Poynting flux is responsible for carrying the energy deep into the magnetosphere. Equation (19) suggests that the energy can reach deeper into the magnetosphere as M_S increases, because $l_{x_{sp}}$ increases with increasing $M_{c_{sp}}$ (<1.0; see Figure 3 of M90). A significant fraction of the energy flux density, which can reach deeper into the magnetosphere than the velocity boundary layer, contributes to compression of magnetic field lines and plasma in the form of a fast magnetosonic wave. The present simulation is performed for a two-dimensional system ($\partial/\partial z = 0$), and there is no resonant field line in the magnetosphere. If a resonant field line exists in the magnetosphere, the fast mode, which penetrates deep into the magnetosphere, will be responsible for an excitation of a ULF pulsation in the magnetosphere by the mechanism of the field line resonance [*Southwood*, 1974; *Chen and Hasegawa*, 1974].

The ionospheric Joule dissipation associated with the Pc 5 toroidal mode resonance is about 6 GW [*Greenwald and Walker*, 1980], which is about 1.5–8.6% of the energy flux required for the viscous interaction. The total energy flux density directed into the magnetosphere at $x \sim 5a$, which is located deeper in the magnetosphere than the VBL, is dominated by the Poynting flux and is about 1/5 of the peak energy flux density at $x \sim 0$ (see Figure 6 of M90). Therefore the energy flux density by the K-H instability which can reach deep into the magnetosphere seems to be large enough to provide energy for the Pc 5 toroidal mode resonance, although the actual energy required for the field line oscillations depends on the position of the resonant field line in the magnetosphere.

The azimuthally polarized transverse Pc 5 waves, which occur predominantly on the morning side of the magnetosphere [*Kokubun*, 1981, 1985; *Takahashi and McPherron*, 1984; *Anderson et al.*, 1990], show a good correlation with ground Pc events [*Kokubun*, 1981]. These waves appear to be fundamental mode resonances and are present almost continuously [*Anderson et al.*, 1990]. *Wolfe et al.* [1980] found a good correlation between the solar wind bulk velocity and the pulsation energy measured on the ground, and *Junginger and Baumjohann* [1988] found a good correlation between Pc 5 power measured at geostationary orbit and the solar wind velocity. These observations suggest that the azimuthally polarized Pc 5 waves with the azimuthal mode number $m < 10$ are fundamental mode toroidal magnetospheric pulsations and are likely to be excited by the field line resonance mechanism, the energy of which is continuously supplied by the K-H instability at the magnetopause. The presence of the substantial Pc 5 activity in the early morning [*Anderson et al.*, 1990] suggests that some of the energy comes from the K-H instability at the tail flank where the magnetosheath flow is supersonic (see Figure 1). Observations by *Junginger and Baumjohann* [1988] showing the saturation of the pulsation amplitude for fast solar wind flows are consistent with the present simulation results (see Figure 2 of M90), which show that for supersonic shear flows the saturation amplitudes of the K-H instability are almost constant for different flow Mach numbers.

For the K-H instability to develop to a finite amplitude a seed perturbation is necessary, and it is perhaps provided by the perturbations in the downstream of the bow shock. Since the dawnside of the magnetosheath flow, which is the downstream of the quasi-parallel shock, is known to be more turbulent than the duskside of the magnetosheath, much larger seed perturbation is expected in the dawnside than in the duskside [*Greenstadt et al.*, 1981]. This may cause an observed dawn-dusk asymmetry of the azimuthally polarized transverse Pc 5 waves.

The original idea of the field line resonance [*Southwood*, 1974; *Chen and Hasegawa*, 1974] assumes a field line resonance driven by a monochromatic source. However, the observational results of *Rostoker and Samson* [1972], *Takahashi and McPherron* [1984], *Anderson et al.* [1989], and *Mitchell et al.* [1990] suggest local resonances in response to a broadband driving source [*Hasegawa et al.*, 1983]. Furthermore, *Takahashi et al.* [1991] found magnetic Pc 4–5 pulsations in the magnetosphere with azimuthal perturbations and position dependent frequency, and they have suggested that these ULF waves are toroidal mode standing Alfvén waves excited by the field line resonance mechanism with a broadband source, which is excited by the K-H instability in the LLBL or at the magnetopause. In the present simulation in which the finite thickness of the velocity shear layer is assumed and the periodicity length in the flow direction is taken equal to the wavelength of the fastest growing mode, only the linearly fastest growing mode is excited in the linear stage (see Figure 2 of *Miura* [1984]). However, in a real situation, all linearly unstable modes with $2k_y a < 2.0$ and $\Delta k_y/k_y \sim 1$ and $\Delta\omega_r/\omega_r \sim 1$ [see *Miura and Pritchett*, 1982, Figures 3 and 4] (this is because ω_r is proportional to k_y for the K-H instability) seem to be excited by the K-H instability. Therefore the actual situation of the field line resonance in the magnetosphere seems to be close to a local resonance in response to a broadband driving source.

Pu and Kivelson [1983*a*, *b*] (see also *Kivelson and Pu* [1984]) calculated the energy flux associated with the linear K-H instability for a zero thickness magnetopause (vortex sheet). Since their calculation was based on the linear analysis, however, they had to assume an amplitude of the developed wave for calculating the energy flux. Furthermore, they did not use a single frame (e.g., the rest frame of the magnetosphere) for calculation of the energy flux, which is frame dependent, and therefore they could not determine the direction of the net energy transfer. Their calculation shows the existence of the net energy transport only when the magnetosheath flow is subfast, because the vortex sheet is stable for the super fast velocity jump. *Mishin and Matyukhin* [1986] also calculated the energy flux associated with the linear K-H instability for a finite thick velocity shear layer and assumed a wave amplitude. Since they were using a finite thick velocity shear layer, their energy flux exists for a supersonic shear flow. However, their calculation of the energy flux also does not seem to be done in a single frame. Owing to the difference of the frames for calculation of the energy flux, comparison of the present results, which were done using the rest frame of the magnetosphere, with their calculations does not seem to be possible.

5.5. *Stability of the Magnetopause and Vortices*

Watanabe and Sato [1990] reported that in their global MHD simulation the K-H instability did not occur at the magnetopause. Since the velocity shear at the magnetopause occurs only in a few spatial meshes in their simulation, the K-H instability does not seem to be realized in their simulation. It should be stressed that if a higher precision code is used in the MHD simulation, the velocity shear transition at the magnetopause occurs in fewer meshes, a dilemma associated with the MHD simulation, which does not include any characteristic plasma length. A fully kinetic, global particle simulation [*Buneman*, 1991] and a global hybrid simulation [*Korzhenevskiy and Cherepenin*, 1991], which can determine the thickness of the velocity shear layer at the magnetopause self-consistently, by kinetic effects, may resolve the above numerical difficulty in the future.

By means of a statistical study of ISEE 1 and 2 multiple crossings, *Song et al.* [1988] have concluded that the K-H instability plays a very minor role in causing the magnetopause oscillations. *Belmont and Chanteur* [1989] argue, however, that their statistical analysis cannot be conclusive, because it did not distinguish between the multiple crossings with short periods (1–10 min) [*Aubry et al.*, 1971], which are considered to be due to the K-H instability, and the more separated crossings (10 min to 1 hour), which are, perhaps, due to the solar wind dynamic pressure fluctuations. From the good correlation between the number of ISEE 3 magnetotail magnetopause crossings and the solar wind/magnetosheath velocities, *Sibeck et al.* [1987] have suggested that the K-H instability drives substantial magnetopause motion in the distant magnetotail.

By checking the linear instability criterion of the incompressible K-H instability for a vortex sheet (zero thickness shear layer), *Ogilvie and Fitzenreiter* [1989] have found that the magnetopause is usually stable but the inner edge of the boundary layer satisfies the linear instability criterion. Consequently, they favored the K-H instability at the inner edge of the boundary layer [*Lee et al.*, 1981] instead of the K-H instability at the magnetopause. Their conclusion does not seem to be conclusive, however, because in addition to the fact that the magnetosheath flow near the dawn-dusk magnetopause is compressible and the velocity shear layer is finite thick, the plasma and magnetic field parameters used in their evaluation may actually represent those at the nonlinear saturation stage of the K-H instability.

McHenry et al. [1990*a*, *b*] found steady, traveling ionospheric convection vortices at the ionospheric convection reversal boundary. During quiet times these periodic vortices consist of a continuous series of vortices moving generally antisunward for several hours at a time. These vortices are on the field lines which map to the inner edge of the low-latitude boundary layer. By studying their relationship with solar wind parameters, *McHenry et al.* [1990*b*] suggest that these vortices are ionospheric signatures of the K-H instability excited at the inner edge of the magnetospheric boundary layer. The fact that a vortex is located at the inner edge of the LLBL, however, does not necessarily mean that the K-H instability is excited there. The present simulation shows that although the velocity shear layer and the magnetopause are overlapped initially, the velocity shear layer diffuses into the magnetosphere by the momentum transport by the K-H instability (see Figure 7). Therefore the vortex ends up at the inner edge of the VBL, although the K-H instability was excited at the initial velocity shear layer at the magnetopause in the present simulation (notice that the VBL is similar to the LLBL as far as the flow momentum is

concerned); this consequence is consistent with their observations. Also the tailward streaming velocity of their observed vortices mapped onto the equatorial plane is comparable to the phase velocity of the K-H wave. In some of their events, the wavelength of the periodic vortices was much longer than the boundary layer thickness [*McHenry et al.*, 1990*b*]. If we remember that the wavelength of the fastest growing mode of the K-H instability is 2π multiplied by the thickness of the velocity shear layer, their observational results do not seem to be in contradiction with the K-H generated vortices. In addition, a fact that the finite compressibility makes the wavelength of the fastest growing mode of the K-H instability longer than the incompressible mode [*Miura and Pritchett*, 1982] favors the K-H interpretation. Furthermore, the nonlinear coalesence of the fastest growing vortices in the nonlinear stage [*Belmont and Chanteur*, 1989], which occurs after the saturation of the fastest growing mode, may explain the observed longer wavelength of the periodic vortices.

As was seen in Figure 7, the vortex is found to be located at the inner edge of the VBL and the streamlines of $E \times B$ velocity presents a wavy pattern inside the inner edge of the VBL. Such a modulation of the inner edge of the VBL may be responsible for the modulations of the energetic particle flux observed by ISEE satellites [*Couzens et al.*, 1985].

6. SUMMARY

For a simple but realistic model of the low-latitude magnetospheric boundary characterized by a velocity shear and gradients of the plasma density and the magnetic field strength normal to the boundary, MHD simulations of the K-H instability have been carried out for different values of the magnetosheath sonic Mach number (M_S). The present work, along with the simulation runs for different magnetosheath Alfvén Mach numbers [*Miura*, 1987], completes a two-dimensional MHD simulation study of the K-H instability for different parameter sets at the low-latitude magnetospheric boundary. Important results obtained by the present simulation study are summarized as follows:

1. For all sonic Mach numbers a velocity boundary layer (VBL) is formed inside the magnetopause owing to the momentum transport by the K-H instability, and it becomes wider for a smaller sonic Mach number. A flow vortex is excited at the inner edge of the VBL for all sonic Mach numbers, and the magnetopause boundary is more highly nonlinearly corrugated by the instability for a smaller sonic Mach number.

2. The energy and momentum flux densities by the instability into the magnetosphere are calculated in the rest frame of the magnetosphere just prior to the saturation of the instability; for $1.0 < M_S < 3.0$ the energy flux density into the magnetosphere is approximated by $0.054\, M_S \rho_0 C_S^3/2 = 0.045 V_0 p_0$, where p_0 is the unperturbed magnetosheath pressure, and the momentum flux density into the magnetosphere or the tangential (shearing) stress at the boundary is approximated by $0.083\, p_0$. The anomalous viscosity by the Reynolds stress associated with the instability decreases in the absolute magnitude with increasing M_S; this suggests that except the subsolar regions where the instability is suppressed by the magnetic tension force, the dayside and the dawn-dusk magnetopauses, where the magnetosheath flow remains subsonic, are the most viscous parts of the boundary, although the tail flank boundaries were also found to be viscous enough for the viscous interaction. The energy flux density into the magnetosphere is large enough to replenish the LLBL with the tailward flow kinetic energy of the observed intensity and the substantial amount of the energy flux density in the form of the Poynting flux penetrates deeper into the magnetosphere than the VBL to excite a ULF wave.

3. For the supersonic magnetosheath convective Mach number the total pressure perturbation δp^* in the magnetosheath becomes oscillatory in the x direction, while in the magnetosphere it is evanescent because the magnetospheric convective Mach number remains less than 1.0.

4. For a sufficiently high sonic Mach number the leading edge of the unstable pressure wave in the magnetosheath steepens nonlinearly and finally develops into a shock, which is a parallel shock in the present magnetosheath configuration where the flow is parallel to the magnetic field. The shock satisfies well the Rankine-Hugoniot relationship for the gasdynamical shock because of $C_S > V_A$.

Acknowledgments. I would like to thank W. Allan, U. Anzer, G. Belmont, D. Burgess, G. Chanteur, C. R. Clauer, G. Haerendel, W. J. Heikkila, J. Lemaire, B. Lembege, R. Lundin, G. Paschmann, G. Rostoker, M. Roth, A. Roux, T. Sato, N. Sckopke, T. Tamao, A. D. M. Walker, and colleagues of the STP group of the DEPP for useful discussions and comments during the course of this study. I would also like to thank J. R. Spreiter for his kind help in making Figure 1 and T. Nakamura for providing some of the plotting routines. Thanks are also due to the referees for constructive comments. This work has been supported by Grants-in-Aid for Scientific Research 63740229 and 03640390, provided by the Japanese Ministry of Education, Science and Culture and, in part, by the Yamada Science Foundation.

The Editor would like to thank G. Chanteur and one other referee for their help in evaluating this paper.

REFERENCES

Allan, W., and E. M. Poulter, The spatial structure of different ULF pulsation types: A review of stare radar results, *Rev. Geophys.*, *22*, 85, 1984.

Anderson, B. J., M. J. Engebretson, and L. J. Zanetti, Distortion effects in spacecraft observations of MHD toroidal standing waves: Theory and observations, *J. Geophys. Res.*, *94*, 13,425, 1989.

Anderson, B. J., M. J. Engebretson, S. P. Rounds, L. J. Zanetti, and T. A. Potemra, A statistical study of Pc 3–5 pulsations observed by the Ampte/CCE magnetic fields experiment, 1, Occurence distributions, *J. Geophys. Res.*, *95*, 10,495, 1990.

Anzer, U., and G. Börner, Accretion by neutron stars: accretion disk and rotating magnetic field, *Astron. Astrophys.*, *83*, 133, 1980.

Arons, J., and S. M. Lea, Accretion onto magnetized neutron stars: The fate of sinking filaments, *Astrophys. J.*, *235*, 1016, 1980.

Atkinson, G., and T. Watanabe, Surface waves on the magnetosphere boundary as a possible origin of long period micropulsations, *Earth Planet Sci. Lett.*, *1*, 89, 1966.

Aubry, M. P., M. G. Kivelson, and C. T. Russell, Motion and structure of the magnetopause, *J. Geophys. Res.*, *76*, 1673, 1971.

Axford, W. I., Viscous interaction between the solar wind and the Earth's magnetosphere, *Planet. Space Sci.*, *12*, 45, 1964.

Axford, W. I., and C. O. Hines, A unifying theory of high-latitude geophysical phenomena and geomagnetic storms, *Can. J. Phys.*, *39*, 1433, 1961.

Baranov, V. B., H. J. Fahr, and M. S. Ruderman, Investigation of macroscopic instabilities at the heliopause boundary surface, paper presented at XXI General Assembly, Eur. Geophys. Soc., Germany, 1991.

Baumjohann, W., and G. Paschmann, Solar wind-magnetosphere coupling processes and observations, *Phys. Scr. T*, *18*, 61, 1987.

Bazer, J., and W. B. Ericson, Hydromagnetic shocks, *Astrophys. J.*, *129*, 758, 1959.

Belmont, G., and G. Chanteur, Advances in magnetopause Kelvin-Helmholtz instability studies, *Phys. Scr.*, *40*, 124, 1989.

Berchem, J., and H. Okuda, A two dimensional particle simulation of the magnetopause current layer, *J. Geophys. Res.*, *95*, 8133, 1990.

Blumen, W., P. G. Drazin, and D. F. Billings, Shear layer instability of an inviscid compressible fluid, 2, *J. Fluid Mech.*, *71*, 305, 1975.

Boller, B. R., and H. L. Stolov, Kelvin-Helmholtz instability and the semiannual variation of geomagnetic activity, *J. Geophys. Res.*, *75*, 6073, 1970.

Buneman, O., Interaction of solar wind and earth's field as simulated by a 3-D E-M particle code, in *Proceedings of the 4th International School for Space Simulation*, edited by H. Matsumoto, p. 5, Kyoto, Japan, 1991.

Cai, D., Particle loadings of a plasma shear layer across a magnetic field, in *Proceedings of the 4th International School for Space Simulation*, edited by H. Matsumoto, p. 109, Kyoto University, Kyoto, Japan, 1991.

Chandrasekhar, S., *Hydrodynamic and Hydromagnetic Stability*, Oxford University Press, New York, 1961.

Chanteur, G., and E. Proteneuve, Vectorization and parallelization of a simulation code for magnetofluid dynamics, in *High Performance Computing*, edited by J.-L. Delhaye and E. Gelenbe, p. 311, Elsevier Science, New York, 1989.

Chen, L., and A. Hasegawa, A theory of long-period magnetic pulsations, 1, Steady state excitation of field line resonance, *J. Geophys. Res.*, *79*, 1024, 1974.

Choudhury, S. R., and R. V. E. Lovelace, On the Kelvin-Helmholtz instabilities of supersonic shear layers, *Astrophys. J.*, *283*, 331, 1984.

Couzens, D. A., G. K. Parks, K. A. Anderson, R. P. Lin, and H. Reme, ISEE particle observations of surface waves at the magnetopause boundary layer, *J. Geophys. Res.*, *90*, 6343, 1985.

Cowley, S. W. H., The causes of convection in the earth's magnetosphere: A review of developments during the IMS, *Rev. Geophys.*, *20*, 531, 1982.

Doyle, M. A., and W. J. Burke, S3-2 measurements of the polar cap potential, *J. Geophys. Res.*, *88*, 9125, 1983.

Drazin, P. G., and A. Davey, Shear layer instability of an inviscid compressible fluid, part 3, *J. Fluid Mech.*, *82*, 255, 1977.

Dungey, J. W., Electrodynamics of the outer atmosphere, in *Proceedings of the Ionosphere Conference*, p. 225, Physical Society of London, 1955.

Eardley, D. M., and A. P. Lightman, Magnetic viscosity in relativistic accretion disks, *Astrophys. J.*, *200*, 187, 1975.

Eastman, T. E., The plasma boundary layer of the Earth's magnetosphere, Ph.D. thesis, Univ. of Alaska, Fairbanks, 1979.

Eastman, T. E., Observation of the magnetospheric boundary layers, in Proceedings of the Conference on Achievements of the International Magnetospheric Study, *Eur. Space Agency Spec. Publ., ESA SP-217*, 77, 1984.

Eastman, T. E., and E. W. Hones, Jr., Characteristics of the magnetospheric boundary layer and magnetopause layer as observed by IMP 6, *J. Geophys. Res.*, *84*, 2019, 1979.

Ershkovich, A. I., and D. A. Mendis, On the penetration of the solar wind into the cometary ionosophere, *Astrophys. J.*, *269*, 743, 1983.

Eviatar, A., and R. W. Wolf, Transfer processes in the magnetopause, *J. Geophys. Res.*, *73*, 5561, 1968.

Fahr, H. J., W. Neutsch, S. Grzedzielski, W. Macek, and R. Ratkiewicz-Landowska, Plasma transport across the heliopause, *Space Sci. Rev.*, *43*, 329, 1986.

Fejer, J. A., Hydromagnetic stability at a fluid velocity discontinuity between compressible fluids, *Phys. Fluids*, *7*, 499, 1964.

Fejer, J. A., and J. W. Miles, On the stability of a plane vortex sheet with respect to three-dimensional disturbances, *J. Fluid Mech.*, *15*, 335, 1963.

Fujimoto, M., and T. Terasawa, On the use of spline functions for differential representations in the hybrid code simulation, in *Proceedings of the 4th International School for Space Simulation*, edited by H. Matsumoto, p. 138, Kyoto University, Kyoto, Japan, 1991*a*.

Fujimoto, M., and T. Terasawa, Ion inertia effect on the Kelvin-Helmholtz instability, *J. Geophys. Res.*, *96*, 15,725, 1991*b*.

Gary, S. P., and T. E. Eastman, The lower hybrid drift instability at the magnetopause, *J. Geophys. Res.*, *84*, 7378, 1979.

Gendrin, R., Magnetic turbulence and diffusion processes in the magnetopause boundary layer, *Geophys. Res. Lett.*, *10*, 769, 1983.

Gerwin, R. A., Stability of the interface between two fluids in relative motion, *Rev. Mod. Phys.*, *40*, 652, 1968.

Ghosh, P., and F. K. Lamb, Accretion by rotating magnetic neutron stars, II, Radial and vertical structure of the transition zone in disk accretion, *Astrophys. J.*, *232*, 259, 1979.

Gill, A. E., Instabilities of "Top-Hat" jets and wakes in compressible fluids, *Phys. Fluids*, *8*, 1428, 1965.

Goldstein, M. L., S. Ghosh, D. A. Roberts, W. H. Matthaeus, and W. T. Stribling, Recent progress in simulating turbulence in compressible and incompressible magnetofluids, *Eos Trans. AGU*, *71*, 913, 1990.

Greenstadt, E. W., R. L. McPherron, and K. Takahashi, Solar wind control of daytime, midperiod geomagnetic pulsations, in *ULF Pulsations in the Magnetosphere*, edited by D. J. Southwood, p. 89, Center for Academic Publications Japan, Tokyo, 1981.

Greenwald, R. A., and A. D. M. Walker, Energetics of long period resonant hydromagnetic waves, *Geophys. Res. Lett.*, *7*, 745, 1980.

Gropengiesser, H., Study of the stability of boundary layers in compressible fluids, *NASA Tech. Note, TT-F-12*, 786, 1970.

Hardee, P. E., Effects of the Kelvin-Helmholtz surface instability on supersonic jets, *Astrophys. J.*, *269*, 94, 1983.

Hardee, P. E., and M. L. Norman, Spatial stability of the slab jet, I, Linearized stability analysis, *Astrophys. J.*, *334*, 70, 1988.

Hasegawa, A., K. H. Tsui, and A. S. Assis, A theory of long period magnetic pulsations, 3, Local field line oscillations, *Geophys. Res. Lett.*, *10*, 765, 1983.

Heikkila, W. J., Impulsive plasma transport through the magnetopause, *Geophys. Res. Lett.*, *9*, 159, 1982.

Heikkila, W. J., Magnetic reconnection, merging, and viscous interaction in the magnetosphere, *Space Sci. Rev.*, *53*, 1, 1990.

Hoffmann, F. de, and E. Teller, Magneto-hydrodynamic shocks, *Phys. Rev.*, *80*, 692, 1950.

Hones, E. W., Jr., J. R. Asbridge, S. J. Bame, M. D. Montgomery, S. Singer, and S.-I. Akasofu, Measurements of magnetotail plasma flow made with Vela 4B, *J. Geophys. Res.*, *77*, 5503, 1972.

Junginger, H., and W. Baumjohann, Dayside long-period magnetospheric pulsations: Solar wind dependence, *J. Geophys. Res.*, *93*, 877, 1988.

Kivelson, M. G., and Z. Y. Pu, The Kelvin-Helmholtz instability on the magnetopause, *Planet. Space Sci.*, *32*, 1335, 1984.

Kokubun, S., Observations of Pc pulsations in the magnetosphere: Satellite-ground correlation, in *ULF Pulsations in the Magnetosphere*, edited by D. J. Southwood, p. 17, Center for Academic Publications Japan, Tokyo, 1981.

Kokubun, S., Statistical character of Pc 5 waves at geostationary orbit, *J. Geomagn. Geoelectr.*, *37*, 759, 1985.

Korzhenevskiy, A. V., and V. A. Cherepenin, Numerical model of global processes in the magnetosphere, *Dokl. Acad. Nauk. SSSR*, *316*, 1096, 1991.

LaBelle, J., and R. A. Treumann, Plasma waves at the dayside magnetopause, *Space Sci. Rev.*, *47*, 175, 1988.

La Belle-Hamer, A. L., Z. F. Fu, and L. C. Lee, A mechanism for patchy reconnection at the dayside magnetopause, *Geophys. Res. Lett.*, 15, 152, 1988.

Lamb, S. H., *Hydrodynamics*, 6th ed., Cambridge University Press, New York, 1945.

Landau, L., Stability of tangential discontinuities in compressible fluid, *Dokl. Akad. Nauk. SSSR*, *44*, 139, 1944.

Lapidus, A., A detached shock calculation by second-order finite differences, *J. Comput. Phys.*, *2*, 154, 1967.

Lee, L. C., R. K. Albano, and J. R. Kan, Kelvin-Helmholtz instability in the magnetopause boundary layer region, *J. Geophys. Res.*, *86*, 54, 1981.

Lele, S., Direct numerical simulation of compressible free shear flows, *AIAA Pap.*, *89-0374*, Jan. 1989.

Lemaire, J., Impulsive penetration of filamentary plasma elements into the magnetospheres of Earth and Jupiter, *Planet. Space Sci.*, *25*, 887, 1977.

Lemaire, J., and M. Roth, Non-steady-state solar wind magnetosphere interaction, *Space Sci. Rev.*, *57*, 59, 1991.

Lepping, R. P., and L. F. Burlaga, Geomagnetopuase surface fluctuations observed by Voyager 1, *J. Geophys. Res.*, *84*, 7099, 1979.

Lerche, I., Validity of the hydromagnetic approach in discussing instability of the magnetospheric boundary, *J. Geophys. Res.*, *71*, 2365, 1966.

Lessen, M., J. A. Fox, and H. M. Zien, On the inviscid stability of the laminar mixing of two parallel streams of a compressible fluid, *J. Fluid Mech.*, *23*, 355, 1965.

Lessen, M., J. A. Fox, and H. M. Zien, Stability of the laminar mixing of two parallel streams with respect to supersonic disturbances, *J. Fluid Mech.*, *25*, 737, 1966.

Lister, G. G., U. Anzer, and G. Börner, Numerical simulations of accretion onto rotating, magnetic neutron stars, in *Computational Techniques and Applications: CTAC-87*, edited by J. Noye and C. Fletcher, p. 427, Elsevier Science, New York, 1988.

Lotko, W., B. U. Ö. Sonnerup, and R. L. Lysak, Nonsteady boundary layer flow including ionospheric drag and parallel electric fields, *J. Geophys. Res.*, *92*, 8635, 1987.

Lundin, R., Processes in the magnetospheric boundary layer, *Phys. Scr. T*, *18*, 85, 1987.

Maezawa, K., and T. Murayama, Solar wind velocity effects on the auroral zone magnetic disturbances, in *Solar Wind Magnetosphere Coupling*, edited by Y. Kamide and J. A. Slavin, p. 59, Terra Scientific, Tokyo, 1986.

McHenry, M. A., C. R. Clauer, E. Friis-Christensen, P. T. Newell, and J. D. Kelly, Ground observations of magnetospheric boundary layer phenomena, *J. Geophys. Res.*, *95*, 14,995, 1990*a*.

McHenry, M. A., C. R. Clauer, and E. Friis-Christensen, Relationship of solar wind parameters to continuous, dayside, high latitude traveling ionospheric convection vortices, *J. Geophys. Res.*, *95*, 15,007, 1990*b*.

Miles, J. W., On the disturbed motion of a plane vortex sheet, *J. Fluid Mech.*, *4*, 538, 1958.

Mishin, V. V., and Y. G. Matyukhin, A Kelvin-Helmholtz instability on the magnetopause as a possible source of wave energy in the earth's magnetosphere, *Geomagn. Aeron.*, Engl. Transl. *26*, 806, 1986.

Mishin, V. V., and A. G. Morozov, On the effect of oblique disturbances on Kelvin-Helmholtz instability at magnetospheric boundary layers and in solar wind, *Planet. Space Sci.*, *31*, 821, 1983.

Mitchell, D. G., F. Kutchko, D. J. Williams, T. E. Eastman, L. A. Frank, and C. T. Russell, An extended study of the low-latitude boundary layer on the dawn and dusk flanks of the magnetosphere, *J. Geophys. Res.*, *92*, 7394, 1987.

Mitchell, D. G., M. J. Engebretson, D. J. Williams, C. A. Cattell, and R. Lundin, Pc 5 pulsations in the outer dawn magnetosphere seen by ISEE 1 and 2, *J. Geophys. Res.*, *85*, 967, 1990.

Miura, A., Nonlinear evolution of the magnetohydrodynamic Kelvin-Helmholtz instability, *Phys. Rev. Lett.*, *49*, 779, 1982.

Miura, A., Anomalous transport by magnetohydrodynamic Kelvin-Helmholtz instabilities in the solar wind—magnetosphere interaction, *J. Geophys. Res.*, *89*, 801, 1984.

Miura, A., Simulation of Kelvin-Helmholtz instability at the magnetospheric boundary, *J. Geophys. Res.*, *92*, 3195, 1987.

Miura, A., Kelvin-Helmholtz instability for supersonic shear flow at the magnetospheric boundary, *Geophys. Res. Lett.*, *17*, 749, 1990.

Miura, A., and P. L. Pritchett, Nonlocal stability analysis of the MHD Kelvin-Helmholtz instability in a compressible plasma, *J. Geophys. Res.*, *87*, 7431, 1982.

Mozer, F. S., Electric field evidence on the viscous interaction at the magnetopause, *Geophys. Res. Lett.*, 11, 135, 1984.

Nakagawa, T., K. Tsuruda, T. Mukai, A. Nishida, A. Matsuoka, H. Hayakawa, and R. Lepping, Magnetosphere under the IMF condition $B_y = B_z = 0$, in *Proceedings of the 20th General Assembly*, p. 385, International Union of Geodesy and Geophysics, Vienna, Austria, 1991.

Nepveu, M., On shear layers in double radio sources, *Astron. Astrophys.*, *84*, 14, 1980.

Nishida, A., Can random reconnection on the magnetopause produce the low latitude boundary layer?, *Geophys. Res. Lett.*, *16*, 227, 1989.

Norman, M. L., and P. E. Hardee, Spatial stability of the slab jet, II, Numerical simulations, *Astrophys. J.*, *334*, 80, 1988.

Norman, M. L., L. Smarr, K.-H. A. Winkler, and M. D. Smith, Structure and dynamics of supersonic jets, *Astron. Astrophys.*, *113*, 285, 1982.

Ogilvie, K. W., and R. J. Fitzenreiter, The Kelvin-Helmholtz instability at the magnetopause and inner boundary layer surface, *J. Geophys. Res.*, *94*, 15,113, 1989.

Ong, R. S. B., and N. Roderick, On the Kelvin-Helmholtz instability of the Earth's magnetopause, *Planet. Space Sci.*, *20*, 1, 1972.

Owen, C. J., and J. A. Slavin, Viscously driven plasma flows in the deep geomagnetic tail, in *Proceedings of the 20th General Assembly*, p. 410, International Union of Geodesy and Geophysics, Vienna, Austria, 1991.

Papamoshou, D., and A. Roshko, The compressible turbulent shear layer: An experimental study, *J. Fluid Mech.*, *197*, 453, 1988.

Parker, E. N., Interaction of the solar wind with the geomagnetic field, *Phys. Fluids*, *1*, 171, 1958.

Phan, T. D., B. U. Ö. Sonnerup, and W. Lotko, Self-consistent model of the low-latitude boundary layer, *J. Geophys. Res.*, *94*, 1281, 1989.

Prialnik, D., A. Eviatar, and A. E. Ershkovich, The effect of plasma compressibility on the Kelvin-Helmholtz instability, *J. Plasma Phys.*, *35*, 209, 1986.

Pritchett, P. L., and F. V. Coroniti, The collisionless macroscopic Kelvin-Helmholtz instability, 1, Transverse electrostatic mode, *J. Geophys. Res.*, *89*, 168, 1984.

Pu, Z. Y., and M. G. Kivelson, Kelvin-Helmholtz instability at the magnetopause: Solution for compressible plasmas, *J. Geophys. Res.*, *88*, 841, 1983*a*.

Pu, Z. Y., and M. G. Kivelson, Kelvin-Helmholtz instability at the magnetopause: Energy flux into the magnetosphere, *J. Geophys. Res.*, *88*, 853, 1983*b*.

Rajaram, R., D. G. Sibeck, and R. W. McEntire, Linear theory of the Kelvin-Helmholtz instability in the low-latitude boundary layer, *J. Geophys. Res.*, *96*, 9615, 1991.

Reiff, P. H., and J. G. Luhmann, Solar wind control of the polar-cap voltage, in *Solar Wind-Magnetosphere Coupling*, edited by Y. Kamide and J. A. Slavin, p. 453, Terra Scientific, Tokyo, 1986.

Reiff, P. H., R. W. Spiro, and T. W. Hill, Dependence of polar cap potential drop on interplanetary parameters, *J. Geophys. Res.*, *86*, 7639, 1981.

Richardson, I. G., C. J. Owen, S. W. H. Cowley, A. B. Galvin, T. R. Sanderson, M. Scholer, J. A. Slavin, and R. D. Zwickl, ISEE 3 observations during the CDAW 8 intervals: Case studies of the distant geomagnetic tail covering a wide range of geomagnetic activity, *J. Geophys. Res.*, *94*, 15,189, 1989.

Richtmyer, R. D., and K. W. Morton, *Difference Methods for Initial Value Problems*, 2nd ed., Wiley-Interscience, New York, 1967.

Rostoker, G., and J. C. Samson, Pc micropulsations with descrete latitude-dependent frequencies, *J. Geophys. Res.*, *77*, 6249, 1972.

Sandham, N. D., and W. C. Reynolds, Compressible mixing layer: Linear theory and direct simulation, *AIAA J.*, *28*, 618, 1990.

Sandham, N. D., and W. C. Reynolds, Three-dimensional simulations of large eddies in the compressible mixing layer, *J. Fluid. Mech.*, *224*, 133, 1991.

Schardt, A. W., K. W. Behannon, R. P. Lepping, J. F. Carbary, A. Eviatar, and G. L. Siscoe, The outer magnetosphere, in *Saturn*, edited by T. Gehrels and M. S. Matthews, p. 416, University of Arizona Press, Tucson, 1984.

Scharlemann, E. T., The fate of matter and angular momentum in disk accretion onto a magnetized neutron star, *Astrophys. J.*, *219*, 617, 1978.

Sckopke, N., G. Paschmann, G. Haerendel, B. U. Ö. Sonnerup, S. J. Bame, T. G. Forbes, E. W. Hones, Jr., and C. T. Russell, Structure of the low-latitude boundary layer, *J. Geophys. Res.*, *86*, 2099, 1981.

Sen, A. K., Effect of compressibility on Kelvin-Helmholtz instability in a plasma, *Phys. Fluids*, *7*, 1293, 1964.

Sen, A. K., Stability of the magnetospheric boundary, *Planet. Space Sci.*, *13*, 131, 1965.

Shakura, N. I., and R. A. Sunyaev, Black holes in binary systems: Observational appearance, *Astron. Astrophys.*, *24*, 337, 1973.

Sibeck, D. G., J. A. Slavin, and E. J. Smith, ISEE-3 magnetopause crossings: Evidence for the Kelvin-Helmholtz instability, in *Magnetotail Physics*, edited by A. T. Y. Lui, p. 73, Johns Hopkins University Press, Baltimore, Md., 1987.

Siscoe, G. L., W. Lotko, and B. U. Ö. Sonnerup, A high-latitude,

low-latitude boundary layer model of the convection current system, *J. Geophys. Res.*, *96*, 3487, 1991.

Song, P., R. C. Elphic, and C. T. Russell, ISEE 1 and 2 observations of the oscillating magnetopause, *Geophys. Res. Lett.*, *15*, 744, 1988.

Sonnerup, B. U. Ö., Theory of the low-latitude boundary layer, *J. Geophys. Res.*, *85*, 2017, 1980.

Southwood, D. J., The hydromagnetic stability of the magnetospheric boundary, *Planet. Space Sci.*, *16*, 587, 1968.

Southwood, D. J., Some features of field line resonances in the magnetosphere, *Planet. Space Sci.*, *22*, 483, 1974.

Southwood, D. J., Magnetopause Kelvin-Helmholtz instability, in *Proceedings of Magnetospheric Boundary Layers Conference*, *Eur. Space Agency Spec. Publ.*, *ESA SP 148*, 357, 1979.

Southwood, D. J., and W. J. Hughes, Theory of hydromagnetic waves in the magnetosphere, *Space Sci. Rev.*, *35*, 301, 1983.

Spreiter, J. R., A. L. Summers, and A. Y. Alksne, Hydromagnetic flow around the magnetosphere, *Planet. Space Sci.*, *14*, 223, 1966.

Tajima, T., and J. N. Lebouef, Kelvin-Helmholtz instability in supersonic and super-Alfvénic fluids, *Phys. Fluids*, *23*, 884, 1980.

Tajima, T., W. Horton, P. J. Morrison, J. Schtkeher, T. Kamimura, and K. Mima, Instabilities and vortex dynamics in shear flow of magnetized plasmas, *Phys. Fluids*, *B*, *3*, 938, 1991.

Takahashi, K., and R. L. McPherron, Standing hydromagnetic waves in the magnetosphere, *Planet. Space Sci.*, *32*, 1343, 1984.

Takahashi, K., D. B. Sibeck, P. T. Newell, and H. E. Spence, ULF waves in the low-latitude boundary layer and their relationship to magnetospheric pulsations: a multisatellite observation, *J. Geophys. Res.*, *96*, 9503, 1991.

Talwar, S. P., Hydromagnetic stability of the magnetospheric boundary, *J. Geophys. Res.*, *69*, 2707, 1964.

Thomas, V. A., and D. Winske, Kinetic simulation of the Kelvin-Helmholtz instability at the Venus ionopause, *Geophys. Res. Lett.*, *18*, 1943, 1991.

Treumann, R. A., J. Labelle, and R. Pottelette, Plasma diffusion at the magnetopause: The case of lower hybrid drift waves, *J. Geophys. Res.*, *96*, 16,009, 1991.

Tsurutani, B. T., and R. M. Thorne, Diffusion processes in the magnetopause boundary layer, *Geophys. Res. Lett.*, *9*, 1247, 1982.

Walker, A. D. M., The Kelvin-Helmholtz instability in the low-latitude boundary layer, *Planet. Space Sci.*, *29*, 1119, 1981.

Wang, Y.-M., and J. A. Robertson, A numerical investigation of the Kelvin-Helmholtz instability in the context of accreting neutron stars, *Astron. Astrophys.*, *139*, 93, 1984.

Watanabe, K., and T. Sato, Global simulation of the solar wind-magentosphere interaction: The importance of its numerical validity, *J. Geophys. Res.*, *95*, 75, 1990.

Wolfe, A., L. J. Lanzerotti, and C. G. Maclennan, Dependence of hydromagnetic energy spectra on solar wind velocity and interplanetary magnetic field direction, *J. Geophys. Res.*, *85*, 114, 1980.

Wolff, R. S., B. E. Goldstein, and C. M. Yeates, The onset and development of Kelvin-Helmholtz instability at the Venus ionopause, *J. Geophys. Res.*, *85*, 7697, 1980.

Wu, C. C., Kelvin-Helmholtz instability at the magnetopause boundary, *J. Geophys. Res.*, *91*, 3042, 1986.

Wygant, J. R., R. B. Torbert, and F. S. Mozer, Comparison of S3-3 polar cap potential drops with the interplanetary magnetic field and models of magnetopause reconnection, *J. Geophys. Res.*, *88*, 5727, 1983.

Zwan, B. J., and R. A. Wolf, Depletion of solar wind plasma near a planetary boundary, *J. Geophys. Res.*, *81*, 1636, 1976.

A. Miura, Department of Earth and Planetary Physics, University of Tokyo, Bunkyo-ku, Tokyo 113, Japan.

(Received July 18, 1991;
revised February 14, 1992;
accepted March 27, 1992.)